

# Joint stochastic localization and applications

Tom Alberts<sup>1</sup>, Yiming Xu<sup>2</sup>, and Qiang Ye<sup>2</sup>

<sup>1</sup>Department of Mathematics, University of Utah

<sup>2</sup>Department of Mathematics, University of Kentucky

June 11, 2025

## Abstract

Stochastic localization is a pathwise analysis technique originating from convex geometry. This paper explores certain algorithmic aspects of stochastic localization as a computational tool. First, we unify various existing stochastic localization schemes and discuss their localization rates and regularization. We then introduce a joint stochastic localization framework for constructing couplings between probability distributions. As an initial application, we extend the optimal couplings between normal distributions under the 2-Wasserstein distance to log-concave distributions and derive a normal approximation result. As a further application, we introduce a family of distributional distances based on the couplings induced by joint stochastic localization. Under a specific choice of the localization process, the induced distance is topologically equivalent to the 2-Wasserstein distance for probability measures supported on a common compact set. Moreover, weighted versions of this distance are related to several statistical divergences commonly used in practice. The proposed distances also motivate new methods for distribution estimation that are of independent interest.

## 1 Introduction

Stochastic localization (SL) is a pathwise analysis technique introduced by Eldan in the study of isoperimetric problems [Eld13]. It extends an earlier deterministic localization scheme for analyzing the mixing time of random walks on convex bodies [LS93]. In recent years, SL has garnered significant attention for its pivotal role in advancing several conjectures in convex geometry, most notably the Kannan–Lovász–Simonovits (KLS) conjecture [KLS95] and Bourgain’s hyperplane conjecture [Bou86b; Bou86a]. See [LV17; Che21; JLV22; KL22] for some recent breakthroughs on the KLS conjecture that leverage SL, while Bourgain’s hyperplane conjecture has been affirmatively resolved only very recently [KL24; Gua24].

Formally, SL is a measure-valued martingale that deforms a probability measure of interest into “simpler” parts that are easier to analyze; a detailed exposition of SL is given in Section 2. Because of the algorithmic nature, SL has also gained traction in more applied domains, offering insights into numerous sampling-related problems such as mixing bounds for Markov chains [CE22], convergence rates for diffusion models [Ben+23], and entropy-efficient measure decompositions [Eld20], to name just a few. Moreover, SL has been utilized to design practical algorithms for sampling from a target distribution in both discrete and continuous settings [Mon23; EAMS22; MW23; Gre+24; Dem+25]. This paper contributes to the algorithmic aspects of SL from a different perspective. In particular, we focus on a joint SL framework for constructing couplings between probability distributions and associated applications.

Coupling is a well-known probabilistic method allowing for the quantitative comparison of unrelated distributions [DH12]. In addition to being an essential tool for studying Markov chains, coupling has also been employed in other areas such as variance reduction [Gla04], quantitative risk management [WW16], and copula modeling [TZ+07]. One relevant application of coupling in this paper concerns its role in defining metrics on the space of probability distributions. For instance, Wasserstein distances between two probability distributions are defined via the minimum transport cost among all possible couplings between them. Constructing a coupling that attains such a minimum typically requires solving an optimization problem, which becomes computationally intensive when repeated calculations are needed. Consequently, constructing couplings with similar dependence structures while retaining computational efficiency can be useful or even necessary in practice. Our coupling method, introduced and analyzed in Sections 4-7 based on an algorithmic joint SL procedure, offers a potential candidate to meet these needs.

The contributions of the paper can be summarized as three-fold:

- We unify various existing SL schemes through a single-parameter parametrization, which we refer to as Eldan’s  $\alpha$ -scheme. We study how  $\alpha$  affects the localization rate of the corresponding SL scheme (Theorem 3.1) and propose a regularized version to improve numerical stability for implementation. Moreover, we analyze the localization rate of the regularized scheme when  $\alpha = \frac{1}{2}$  and prove an informative bound when the underlying probability distribution is log-concave (Theorem 3.3).
- We introduce a flexible joint SL framework for constructing couplings between probability distributions. As an initial application, we extrapolate the optimal coupling between normal distributions under the 2-Wasserstein distance to log-concave distributions. Although the coupling may no longer remain optimal, it captures a nontrivial dependence structure and implies an upper bound on the 2-Wasserstein distance between strongly log-concave and normal distributions (Theorem 4.2).
- We consider a joint version of Eldan’s  $\alpha$ -scheme within the proposed joint SL framework. The coupling produced by joint Eldan’s  $\alpha$ -scheme induces a distance between probability distributions, which we call the  $\alpha$ -SL distance. We prove that when  $\alpha = 0$ , the corresponding 0-SL distance is topologically equivalent to the 2-Wasserstein distance for distributions defined on a common compact set (Theorem 5.4). Moreover, its weighted variants are related to other statistical divergences such as the Gaussian Kullback–Leibler (KL) divergence (Theorem 6.1) and the score-matching objectives (weighted sums of Fisher divergence) used in training diffusion models (Theorem 6.3). The  $\alpha$ -SL distance also gives rise to new methods for approximating or learning an unknown distribution, for which we provide a numerical procedure for implementation.

In contrast to Wasserstein distances, the  $\alpha$ -SL distance can be estimated via Monte Carlo (MC) simulation of the associated SL process. This explicit construction makes it a promising substitute in applications involving repeated evaluations of Wasserstein distances, such as Generative Adversarial Networks (GANs) [Goo+14] with transport-based distances [ACB17; GPC18; Sal+18]. Alternative metrics, such as sliced Wasserstein distances [Bon+15], share similar computational convenience and topological equivalence properties [Bon13; Nad+19; BG21] but utilize rather different ideas based on random projections to match marginal information.

The rest of the paper is organized as follows. Section 2 reviews SL from two complementary perspectives, including a commonly used formulation and an alternative Bayesian interpretation. Section 3 introduces Eldan’s  $\alpha$ -scheme and discusses its localization rate; a regularized version is

considered and analyzed when  $\alpha = \frac{1}{2}$ . Section 4 presents a joint SL framework for constructing couplings between probability distributions. Building on this, we extend the optimal coupling between normal distributions under the 2-Wasserstein distance to log-concave distributions and obtain a normal approximation result. Section 5 introduces a family of distances induced by joint Eldan's  $\alpha$ -scheme and investigates their properties. Section 6 further relates the distances proposed in Section 5 to several statistical divergences. Section 7 proposes a new method for distribution estimation and discusses its numerical implementation. Section 8 contains several numerical simulations to support our theoretical findings. Section 9 summarizes the results and discusses some future directions.

## 2 Stochastic localization

We first introduce SL following the technical overview [Eld22]. We then present an alternative Bayesian perspective that expands on [KP23, Remark 4.2 (ii)] to provide some additional intuition.

### 2.1 A measure-valued random process

Let  $\mu$  be a probability measure on  $\mathbb{R}^d$ . Let  $W_t$  be a standard Brownian motion in  $\mathbb{R}^d$  with filtration  $\mathcal{F}_t$ . An SL scheme associated with  $\mu$  is a measure-valued stochastic process  $\mu_t$  that is absolutely continuous with respect to  $\mu$  (denoted as  $\mu_t \ll \mu$ ), with its density satisfying the following stochastic differential equations (SDEs):

$$\begin{cases} dp_t(x) &= p_t(x) \langle x - a_t, C_t dW_t \rangle \\ p_0(x) &= 1 \end{cases} \quad x \in \text{supp}(\mu) \quad (2.1)$$

where  $\langle \cdot, \cdot \rangle$  denotes the standard inner product on  $\mathbb{R}^d$ ,

$$a_t = \int_{\mathbb{R}^d} x \mu_t(dx) = \int_{\mathbb{R}^d} x p_t(x) \mu(dx) \quad (2.2)$$

denotes the mean of  $\mu_t$ , and  $C_t \in \mathbb{R}^{d \times d}$  is an  $\mathcal{F}_t$ -adapted matrix-valued control process (i.e., typically it is a matrix-valued function of  $\mu_t$ ).

Note that (2.1) is an infinite system of SDEs if  $\text{supp}(\mu)$  is infinite. Under such circumstances, it is not immediately clear whether (2.1) has a well-defined solution. Fortunately, a series of works [Eld13; EMZ20] have shown that, under suitable regularity assumptions on  $\mu$  and  $C_t$ , (2.1) has a unique solution. We will return to this issue later in Section 3. For now, let us assume that (2.1) has a solution and derive a few consequences from it.

First, note that  $p_t$  is a density a.s. since (i)  $p_t$  is nonnegative if started nonnegative and (ii)

$$d\mu_t(\mathbb{R}^d) = \int_{\mathbb{R}^d} p_t(x) \langle x - a_t, C_t dW_t \rangle \mu(dx) = 0. \quad (2.3)$$

Applying Itô's formula to  $\log p_t(x)$  and using (2.1),

$$d \log p_t(x) = \langle x - a_t, C_t dW_t \rangle - \frac{1}{2} \|C_t^\top (x - a_t)\|_2^2 dt, \quad (2.4)$$

which combined with (2.3) implies

$$p_t(x) = \frac{\exp \left\{ \langle \theta_t, x \rangle - \frac{1}{2} \langle x, G_t x \rangle \right\}}{\int_{\mathbb{R}^d} \exp \left\{ \langle \theta_t, z \rangle - \frac{1}{2} \langle z, G_t z \rangle \right\} \mu(dz)}, \quad (2.5)$$

where

$$\begin{cases} d\theta_t &= C_t C_t^\top a_t dt + C_t dW_t \\ dG_t &= C_t C_t^\top dt \end{cases}. \quad (2.6)$$

We refer to the processes  $\theta_t$  and  $a_t$  as the *observation process* and the *posterior mean process* of the SL scheme (2.1), respectively, for reasons that will become clear in Section 2.2.

Formula (2.5) shows that  $\mu_t$  is a random Gaussian tilt of  $\mu$ . In the special case  $C_t = I$ ,  $G_t = tI$  so that  $p_t$  becomes increasingly spiked on  $\text{supp}(\mu)$ . This implies that  $\mu_t$  converges to a random point mass as  $t \rightarrow \infty$ , which justifies the name “stochastic localization”. Moreover, the converged point mass has the same distribution as  $\mu$  thanks to the martingale structure (see the next paragraph). Such observations inspired practical algorithms to sample from a target distribution by running an SL process (or its observation process  $\theta_t$ ), for target distributions based on the Sherrington–Kirkpatrick (SK) Gibbs measure [EAMS22], spiked models [MW23], nonconvex perceptron models [Dem+25], and other multimodal distributions [Gre+24].

More generally, for any test function  $\varphi : \text{supp}(\mu) \rightarrow \mathbb{R}$  and  $x \in \text{supp}(\mu)$ ,  $\varphi(x)p_t(x)$  is a martingale by Doob’s theorem. Consequently,  $\mathbb{E}_{\mu_t}[\varphi] = \int_{\mathbb{R}^d} \varphi(x) \mu_t(dx) = \int_{\mathbb{R}^d} \varphi(x) p_t(x) \mu(dx)$  is also a martingale. Taking  $\varphi = \mathbb{I}_A$  the indicator function on any Borel set  $A \subseteq \mathbb{R}^d$  and a stopping time  $T$ , the optional stopping theorem implies that  $\mathbb{E}[\mu_T(A)] = \mu(A)$ , thereby decomposing  $\mu$  as a mixture of  $\mu_T$ . In applications,  $C_t$  and  $T$  are often chosen so that  $\mu_T$  is either a point mass or supported on some low-dimensional subspace with prescribed properties [Eld20; EKZ22].

## 2.2 A Bayesian perspective

In the original work of Eldan [Eld13] and a subsequent work [EMZ20], an SL scheme is defined by first specifying  $\theta_t, G_t$  (or some equivalent variants) in (2.6) and then defining SL using (2.5) (as a smooth function of  $\theta_t, G_t$  indexed by  $x$ ). It is thus helpful to get more intuition about the processes  $\theta_t$  and  $G_t$ . With benign abuse of notation, we keep the same notations as before but define them from a different perspective.

Let  $X \sim \mu$  and  $W_t$  be a standard Brownian motion in  $\mathbb{R}^d$  independent of  $X$ . Consider an observation process  $\theta_t$  defined by the following SDE:

$$d\theta_t = C_t C_t^\top X dt + C_t dW_t, \quad (2.7)$$

where  $C_t = C(t, \theta_t) \in \mathbb{R}^{d \times d}$  is a continuous matrix-valued function. Alternative observation processes with deterministic diffusion terms have been considered in [Gre+24].

One may think of (2.7) appearing in a scenario where  $X$  can only be observed through some observation process  $\theta_t$ . See Figure 1 for an illustration where  $C_t = I$  and  $\theta_t = tX + W_t$ . Since the drift in (2.7) is not adapted to  $W_t$ , one cannot simulate  $\theta_t$  due to the lack of knowledge of  $X$ . Fortunately, we can apply a time-dependent variant of [Øks03, Theorem 8.4.3] to obtain an Itô diffusion that has the same law as (2.7):

$$\begin{cases} d\theta_t &= C_t C_t^\top \mathbb{E}[X \mid \mathcal{G}_t] dt + C_t dW_t \\ \theta_0 &= 0 \end{cases}, \quad (2.8)$$

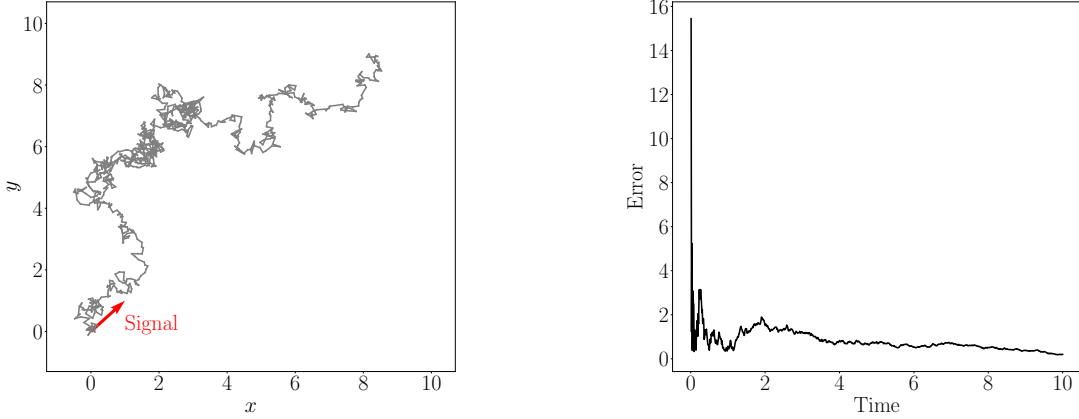


**Figure 1:** A trajectory of the observation process  $\theta_t = tX + W_t$  with  $X = (1, 1)^\top$  (left). As  $t$  grows, the signal-to-noise ratio increases and thus  $\theta_t$  becomes increasingly informative of the unobserved signal  $X$ . This can be measured by computing the  $\ell_2$  distance (error) between the normalized signal  $\frac{\theta_t}{t}$  and  $X$  (right).

where  $\mathcal{G}_t$  is the filtration generated by  $\theta_t$ .

Viewing (2.7) from a Bayesian perspective, one can consider an associated filtering problem of computing the posterior distribution of  $X$  given  $\mathcal{G}_t$  using Bayes' formula. In the finite-dimensional setting, the posterior distribution of a random vector  $Z_1 \in \mathbb{R}^{d_1}$  given a coupled observation  $Z_2 \in \mathbb{R}^{d_2}$  is proportional to their joint density  $p(z_1, z_2)$  with respect to the Lebesgue measure on  $\mathbb{R}^{d_1+d_2}$  (provided it exists). This can be generalized to other scenarios by replacing Lebesgue measure with an appropriate reference measure. In our setting, the probability space is the product space  $\mathbb{R}^d \times C(\mathbb{R}_+, \mathbb{R}^d)$  ( $C(\mathbb{R}_+, \mathbb{R}^d)$  is equipped with the Borel  $\sigma$ -algebra associated with the topology of uniform convergence on every compact set). One can take the reference measure as the product measure  $\mu(dx) \otimes \mathcal{L}_{\theta'_t}(d\omega)$ , where  $\mathcal{L}_{\theta'_t}(d\omega)$  is the law of the diffusion process  $d\theta'_t = C_t dW_t$ . Let  $\mathcal{L}_{x, \theta_t}(dx, d\omega)$  be the joint distribution of  $X$  and  $\{\theta_s\}_{0 \leq s \leq t}$ . Under suitable regularity assumptions on  $C_t$ ,  $\mathcal{L}_{x, \theta_t}(dx, d\omega)$  is absolutely continuous with respect to  $\mu(dx) \otimes \mathcal{L}_{\theta'_t}(d\omega)$  and the Radon–Nikodym derivative can be computed using a version of Girsanov's theorem [Øks03, Theorem 8.6.8]:

$$\begin{aligned} \frac{d\mathcal{L}_{x, \theta_t}(dx, d\omega)}{d(\mu(dx) \otimes \mathcal{L}_{\theta'_t}(d\omega))} \Big|_{x, \{\theta_s\}_{0 \leq s \leq t}} &= \exp \left\{ \frac{1}{2} \langle x, G_t x \rangle + \left\langle \int_0^t C_s dW_s, x \right\rangle \right\} \\ &\stackrel{(2.7)}{=} \exp \left\{ \langle \theta_t, x \rangle - \frac{1}{2} \langle x, G_t x \rangle \right\}, \end{aligned} \quad (2.9)$$

where  $G_t = \int_0^t C_s C_s^\top ds$ . If we denote the conditional distribution of  $X$  on  $\mathcal{G}_t$  as  $\mu_t$ , then an application of Bayes' formula yields

$$\mu_t(dx) = \frac{\exp \left\{ \langle \theta_t, x \rangle - \frac{1}{2} \langle x, G_t x \rangle \right\} \mu(dx) \mathcal{L}_{\theta'_t}(d\omega)}{\int_{\mathbb{R}^d} \exp \left\{ \langle \theta_t, z \rangle - \frac{1}{2} \langle z, G_t z \rangle \right\} \mu(dz) \mathcal{L}_{\theta'_t}(d\omega)}, \quad (2.10)$$

which agrees with the solution to the SL scheme in (2.1).

**Remark 2.1.** The above derivations suggest that an SL process  $\mu_t$  associated with  $\mu$  can be interpreted as the posterior distribution of  $X$  conditional on the observation process  $\theta_s$  up to

time  $t$ . Similarly, the process  $a_t$  can be interpreted as the posterior mean of  $X$ . In general,  $a_t$  depends on the whole trajectory  $\{\theta_s\}_{0 \leq s \leq t}$ . When  $C_t = I$ ,  $a_t$  is a deterministic function of the terminal point  $\theta_t$  only, i.e.,  $a_t = a_t(\theta_t)$ . Moreover, if  $\mu$  is absolutely continuous with respect to the Gaussian measure on  $\mathbb{R}^d$ , then  $\theta_t$  is equal to a rescaled Föllmer process associated with  $\mu$ . We will come back to this in Section 6.1.

### 3 Control processes

The properties of an SL scheme depend on the control process  $C_t$ , and different choices of  $C_t$  have been used in various applications. For instance,  $C_t = I$  was used in a series of breakthroughs on the KLS conjecture [LV17; Che21; JLV22; KL22] and Bourgain’s hyperplane conjecture [KL24; Gua24], as well as other works that utilize SL as sampling algorithms [EAMS22; MW23; Gre+24; Dem+25]. An algorithmic advantage of this choice is that simulating  $\theta_t$  requires only the first-order information of the posterior distribution  $\mu_t$  and is thus relatively easy to implement, especially when  $d$  is large.

In Eldan’s original work [Eld13],  $C_t = \Sigma_t^{-\frac{1}{2}}$  was used to isotropize the SL dynamics, where  $\Sigma_t = \int_{\mathbb{R}^d} (x - a_t)^{\otimes 2} \mu_t(dx)$  is the covariance of  $\mu_t$ . Since  $\Sigma_t$  is shrinking on average (e.g., see Theorem 3.1), it is unclear whether  $C_t$  is well-defined for all finite time. In the same work, Eldan showed that for all log-concave distributions,  $\Sigma_t$  is nonsingular for  $t \geq 0$  a.s., so the unique existence of SL is guaranteed. The proof relies on a rescaling property of log-concave distributions.

In subsequent works on Skorokhod embedding [Eld16; EMZ20], a more extreme choice  $C_t = \Sigma_t^\dagger$  was employed, where  $\dagger$  denotes the pseudoinverse. They aimed to embed  $\mu$  as a stopped Brownian motion so that  $\Sigma_t$  vanishes within a finite time. Importantly, they showed that as long as  $\mu$  is bounded and has a smooth density and  $C_t$  has a continuous dependence on  $\Sigma_t^\dagger$  and  $t$ , the corresponding SL process is well-defined for all  $t > 0$  via an induction argument. In particular, whenever  $\mu_t$  becomes degenerate, it is supported on a lower-dimensional subspace, as ensured by the regularity assumption on  $\mu$ , and a new SL process can be defined within that subspace. This procedure is repeated until  $\mu_t$  becomes fully localized; see [EMZ20, Section 2.3] for additional details. Besides the abovementioned choices of  $C_t$ , there are more abstract constructions based on smoothened projections [EKZ22].

#### 3.1 Eldan’s $\alpha$ -scheme and localization rates

Motivated by the existing choices, we consider a family of SL schemes with control process  $C_t$  defined as some power of  $\Sigma_t^\dagger$  as follows. Given  $0 \leq \alpha \leq 1$ , define

$$C_t = (\Sigma_t^\dagger)^\alpha. \quad (3.1)$$

We call the SL scheme associated with (3.1) an *Eldan’s  $\alpha$ -scheme*. Previously mentioned schemes are special cases where  $\alpha = 0, \frac{1}{2}$ , and 1.

A natural question one may ask is how  $\alpha$  affects the corresponding SL scheme. One may approach this question from many different angles. Since our focus is on the algorithmic aspect, we consider the average speed of localization as measured by  $\mathbb{E}[\text{tr}(\Sigma_t)]$ .

**Theorem 3.1** (Localization rate of Eldan’s  $\alpha$ -scheme). *Let  $\mu$  be a probability measure on  $\mathbb{R}^d$  with bounded support and a smooth density, and let  $\alpha \in [0, 1]$ . Then the SL scheme (2.1) with  $C_t$  defined in (3.1) has a unique solution. Moreover,*

(i) If  $0 \leq \alpha < \frac{1}{2}$ , then

$$\mathbb{E}[\text{tr}(\Sigma_t)] \leq \left[ \frac{(1-2\alpha)t}{d^{1-2\alpha}} + \frac{1}{\text{tr}(\Sigma_0)^{1-2\alpha}} \right]^{-\frac{1}{1-2\alpha}} \leq \frac{d}{[(1-2\alpha)t]^{\frac{1}{1-2\alpha}} + \frac{d}{\text{tr}(\Sigma_0)}};$$

(ii) If  $\alpha = \frac{1}{2}$ , then  $\mathbb{E}[\text{tr}(\Sigma_t)] = \text{tr}(\Sigma_0)e^{-t}$ ;

(iii) If  $\frac{1}{2} < \alpha \leq 1$ , then there exists a deterministic time  $T(\alpha) < \infty$  such that  $\Sigma_t = 0$  for all  $t \geq T(\alpha)$ .

**Remark 3.2.** The smooth density assumption is only needed for the existence of the SL scheme for all  $\alpha \in [0, 1]$ . There are other scenarios where Theorem 3.1 remains valid; for instance, when  $\mu$  has finite support (i.e., the same induction argument in [EMZ20, Proposition 1] applies almost verbatim). This is relevant to the applications considered in Sections 7-8. On the other hand, if  $\alpha = 0$ , then assuming  $\mu$  has a bounded first moment is sufficient [LS77, Theorem 7.1.2]. We will use this fact in the discussion in Section 5.2.

Theorem 3.1 generalizes similar results for the cases  $\alpha = 0$  [Eld20] and  $\alpha = \frac{1}{2}$  [EL14]. The proof relies on applying Itô's formula to the moment statistics of  $\mu_t$ . As these formulas will be used frequently throughout the paper, we derive them below before proceeding to the proof. We first derive the dynamics of the posterior mean process  $a_t$ :

$$\begin{aligned} da_t &= \int_{\mathbb{R}^d} x dp_t(x) \mu(dx) \\ &\stackrel{(2.1)}{=} \int_{\mathbb{R}^d} x \otimes (x - a_t) p_t(x) \mu(dx) C_t dW_t \\ &= \int_{\mathbb{R}^d} (x - a_t) \otimes (x - a_t) \mu_t(dx) C_t dW_t \\ &= \Sigma_t C_t dW_t. \end{aligned} \tag{3.2}$$

Note that  $a_t$  is a martingale (since  $\mu$  has bounded support) with its quadratic variation process given by

$$d[a_t \otimes a_t] = \Sigma_t C_t C_t^\top \Sigma_t dt. \tag{3.3}$$

We also compute the dynamics of  $\Sigma_t$  as follows:

$$d\Sigma_t = -\Sigma_t C_t C_t^\top \Sigma_t dt + \mathcal{M}^{(3)}[\mu_t] C_t dW_t, \tag{3.4}$$

where  $\mathcal{M}^{(3)}[\mu_t] = \int_{\mathbb{R}^d} (x - a_t)^{\otimes 3} \mu_t(dx)$  denotes the third-order centered tensorial moment of  $\mu_t$ . These computations suggest a moment-generating property of SL: understanding the dynamics of the  $k$ th moments of  $\mu_t$  requires information on the  $(k+1)$ st moment.

*Proof of Theorem 3.1.* Under the assumptions, the unique existence of Eldan's  $\alpha$ -scheme follows from [EMZ20, Propositions 1-2]. Therefore, it remains to check the convergence rate of  $\Sigma_t$ . Note that under the choice  $C_t = [\Sigma_t^\dagger]^\alpha$  and the boundedness assumption, the diffusion term in (3.4) is a martingale started from the zero matrix. Taking trace and then expectation on both sides yields

$$d\mathbb{E}[\text{tr}(\Sigma_t)] = -\mathbb{E}[\text{tr}(\Sigma_t^{2-2\alpha})] dt.$$



Since  $x \mapsto x^p$  is operator convex for  $p \geq 1$ ,  $\mathbb{E}[\Sigma_t^{2-2\alpha}] \succeq \mathbb{E}[\Sigma_t]^{2-2\alpha}$  when  $0 \leq \alpha \leq \frac{1}{2}$ . Consequently,

$$-\mathbb{E}[\text{tr}(\Sigma_t^{2-2\alpha})] \leq -\text{tr}(\mathbb{E}[\Sigma_t]^{2-2\alpha}) \leq -\frac{\mathbb{E}[\text{tr}(\Sigma_t)]^{2-2\alpha}}{d^{1-2\alpha}},$$

where the second step follows from Jensen's inequality applied to the spectrum of  $\mathbb{E}[\Sigma_t]$ . On the other hand, when  $\frac{1}{2} < \alpha \leq 1$ ,  $0 \leq 2 - 2\alpha < 1$  so that

$$-\mathbb{E}[\text{tr}(\Sigma_t^{2-2\alpha})] \leq -\mathbb{E}[\text{tr}(\Sigma_t)^{2-2\alpha}] \lesssim -\mathbb{E}[\text{tr}(\Sigma_t)]^{2-2\alpha},$$

where the last inequality requires the boundedness assumption of  $\mu$  (which implies that  $\text{tr}(\Sigma_t)$  is uniformly bounded for all  $t$ ). The desired results follow from a Grönwall type estimate applied to  $t \mapsto e^{-\mathbb{E}[\text{tr}(\Sigma_t)]^{2\alpha-1}}$  for  $\alpha \neq \frac{1}{2}$  and directly solving the equation for  $\alpha = \frac{1}{2}$ .  $\square$

### 3.2 Regularized Eldan's $\alpha$ -scheme

Theorem 3.1 shows that larger values of  $\alpha$  correspond to faster convergence. When  $\alpha > \frac{1}{2}$ , localization occurs within uniformly finite time a.s., which implies singularity when simulating  $\Sigma_t^\dagger$ . Moreover, their corresponding joint SL schemes induce “degraded” couplings in terms of transport cost; see Section 8.2 for some empirical evidence. As such, we will mainly focus on the case  $0 \leq \alpha \leq \frac{1}{2}$  in the rest of the paper.

When  $0 < \alpha \leq \frac{1}{2}$ , even though  $\mathbb{E}[\Sigma_t]$  remains positive for  $t \geq 0$ ,  $\Sigma_t$  may vanish in (nonuniformly) finite time a.s., which again poses numerical instability.

**Example 1** (Finite-time localization of Eldan's  $\frac{1}{2}$ -scheme). Let  $\mu = \frac{1}{2}\delta_0 + \frac{1}{2}\delta_1$  denote the unbiased Bernoulli distribution and consider its associated Eldan's  $\frac{1}{2}$ -scheme  $\mu_t$ . In this case,  $\mu_t$  is determined by  $p_t(x)$  at  $x = 1$  (denoted by  $p_t$ ) which satisfies  $dp_t = \sqrt{2p_t - p_t^2} dW_t$  and  $p_0 = 1$ . This is a special case of the Wright–Fisher diffusion with an absorbing boundary [Dur18, Exercise 5.5]. For this diffusion, it is known that  $p_t$  hits either 0 or 2 in finite time a.s.

To address this issue, we add a small multiple of the identity matrix to  $\Sigma_t$ . The rest of this section aims to understand the impact of regularization on the localization rate. We focus on the case  $\alpha = \frac{1}{2}$  as this is often the preferred choice in practice for accelerating convergence.

Fix  $\delta < 1$  as a regularization parameter. Consider the  $\delta$ -regularized Eldan's  $\frac{1}{2}$ -scheme with

$$C_t = [\Sigma_t(\delta)]^{-\frac{1}{2}} \quad \Sigma_t(\delta) = \Sigma_t + \delta I. \quad (3.5)$$

When  $\mu$  has bounded support, the condition number of  $C_t$  is bounded by  $\mathcal{O}(\delta^{-\frac{1}{2}})$ , so a large  $\delta$  yields better numerical stability. On the other hand, too large a value of  $\delta$  may slow down the localization rate. This is because when  $\text{tr}(\Sigma_t) \leq \delta$ , the regularized SL scheme resembles Eldan's 0-scheme. This observation can be made rigorous for log-concave distributions using a pathwise analysis empowered by SL.

**Definition 1** (Log-concave distributions on  $\mathbb{R}^d$ ). A (nondegenerate) probability measure  $\mu$  on  $\mathbb{R}^d$  is called log-concave if  $\mu$  has a density  $p$  with respect to the Lebesgue measure on  $\mathbb{R}^d$  such that  $\log p$  is a concave function. Moreover, it is called  $\kappa$ -strongly log-concave for some  $\kappa > 0$  if  $\nabla^2 \log p \preceq -\kappa I$ .



**Theorem 3.3.** *Let  $\mu$  be a probability measure on  $\mathbb{R}^d$  and  $\delta > 0$ . If  $\text{diam}(\text{supp}(\mu)) \leq R$  for some  $R > 0$ , then the  $\delta$ -regularized Eldan's  $\frac{1}{2}$ -scheme  $\mu_t$  exists for all  $t \geq 0$ , and its covariance  $\Sigma_t$  satisfies  $\mathbb{E}[\text{tr}(\Sigma_t)] \leq \frac{d(R^2 + \delta)}{t}$ . Moreover, if  $\mu$  is log-concave, then for all small  $\delta$ ,  $\mathbb{E}[\text{tr}(\Sigma_t)] \leq \text{tr}(\Sigma_0)e^{-ct}$  for  $t \leq c' \log(\frac{1}{d\delta})$ , where  $c > 0$  is an absolute constant and  $c' > 0$  depends only on  $d$ .*

*Proof.* When  $\mu$  has bounded support,  $C_t$  remains uniformly bounded for all  $t$ . The existence of  $\mu_t$  follows from the standard existence and uniqueness theorem of SDEs [Øks03, Theorem 5.2.1]. It remains to verify the bounds on the localization rate.

The proof for the general bounded support case is similar to Theorem 3.1. Taking the expectation and trace on both sides of (3.4) yields

$$d\mathbb{E}[\text{tr}(\Sigma_t)] = -\mathbb{E}[\text{tr}(\Sigma_t^2 \Sigma_t^{-1}(\delta))] dt. \quad (3.6)$$

Under the assumption  $\text{diam}(\text{supp}(\mu)) \leq R$ ,  $\|\Sigma_t(\delta)\|_2 \leq R^2 + \delta$ , so that

$$\mathbb{E}[\text{tr}(\Sigma_t^2 \Sigma_t^{-1}(\delta))] \geq \frac{\text{tr}(\mathbb{E}[\Sigma_t^2])}{R^2 + \delta} \geq \frac{\mathbb{E}[\text{tr}(\Sigma_t)]^2}{d(R^2 + \delta)}. \quad (3.7)$$

Substituting (3.7) into (3.6) and applying a Grönwall type estimate yields that

$$\mathbb{E}[\text{tr}(\Sigma_t)] \leq \frac{d(R^2 + \delta)}{t}.$$

Under the log-concavity assumption, we can improve the error bound in (3.7) via a pathwise analysis. Assume  $d\delta < \min\{\frac{1}{4}, \text{tr}(\Sigma_0)^2\}$  and let  $\tau = \inf\{s : \text{tr}(\Sigma_s) = d\delta\}$  denote the first hitting time of  $\text{tr}(\Sigma_t)$  to  $d\delta$ . Indeed, (3.6) implies that

$$\begin{aligned} d\mathbb{E}[\text{tr}(\Sigma_t)] &\leq -\mathbb{E}[\text{tr}(\Sigma_t^2 \Sigma_t^{-1}(\delta)); \text{tr}(\Sigma_t) \geq d\delta] dt \\ &= -\mathbb{P}(\text{tr}(\Sigma_t) \geq d\delta) \mathbb{E}[\text{tr}(\Sigma_t^2 \Sigma_t^{-1}(\delta)) \mid \text{tr}(\Sigma_t) \geq d\delta] dt \\ &\leq -\frac{1}{6} \mathbb{P}(\text{tr}(\Sigma_t) \geq d\delta) \mathbb{E}[\text{tr}(\Sigma_t) \mid \text{tr}(\Sigma_t) \geq d\delta] dt \\ &\leq -\frac{1}{6} \mathbb{P}(\text{tr}(\Sigma_t) \geq d\delta) \mathbb{E}[\text{tr}(\Sigma_t)] dt \\ &\leq -\frac{1}{6} \mathbb{P}(\tau \geq t) \mathbb{E}[\text{tr}(\Sigma_t)] dt. \end{aligned} \quad (3.8)$$

The second inequality follows from the observation that, if we denote the eigenvalues of  $\Sigma_t$  as  $\lambda_1, \dots, \lambda_d$ , then

$$\sum_{i: \lambda_i \geq \frac{\delta}{2}} \lambda_i \geq \text{tr}(\Sigma_t) - \frac{d\delta}{2} \geq \frac{1}{2} \text{tr}(\Sigma_t) \quad \text{if} \quad \text{tr}(\Sigma_t) \geq d\delta,$$

which further implies

$$\text{tr}(\Sigma_t^2 \Sigma_t^{-1}(\delta)) = \sum_{i=1}^d \frac{\lambda_i^2}{\lambda_i + \delta} \geq \sum_{i: \lambda_i \geq \frac{\delta}{2}} \frac{\lambda_i^2}{\lambda_i + \delta} \geq \frac{1}{3} \sum_{i: \lambda_i \geq \frac{\delta}{2}} \lambda_i \geq \frac{1}{6} \text{tr}(\Sigma_t).$$

Since  $\mathbb{P}(\tau \geq t)$  is nonincreasing in  $t$ , for any  $T > 0$ , the last line of (3.8) can be upper bounded to give

$$d\mathbb{E}[\text{tr}(\Sigma_t)] \leq -\frac{1}{6} \mathbb{P}(\tau \geq T) \mathbb{E}[\text{tr}(\Sigma_t)] dt$$

for all  $t \leq T$ . We will show that there exists a constant  $c_0 = c_0(d) > 0$ , depending only on  $d$ , such that if  $T = \frac{\log(\frac{1}{d\delta})}{2(2+c_0)}$  then  $\mathbb{P}(\tau \geq T) > \frac{3}{10}$ , so that the above becomes

$$d\mathbb{E}[\text{tr}(\Sigma_t)] \leq -\frac{1}{20}\mathbb{E}[\text{tr}(\Sigma_t)] dt$$

for all  $t \leq T$ . Thus  $\mathbb{E}[\text{tr}(\Sigma_t)] \leq \text{tr}(\Sigma_0)e^{-\frac{t}{20}}$  for all  $t \leq \frac{\log(\frac{1}{d\delta})}{2(2+c_0)}$ . Taking  $c = \frac{1}{20}$  and  $c' = \frac{1}{2(2+c_0)}$  will complete the proof.

It only remains to show that there exists a constant  $c_0 = c_0(d)$  such that if  $T = \frac{\log(\frac{1}{d\delta})}{2(2+c_0)}$  then  $\mathbb{P}(\tau \geq T) > \frac{3}{10}$ . To this end, we take the trace on both sides of (3.4) without taking expectation:

$$d\text{tr}(\Sigma_t) = -\text{tr}(\Sigma_t^2 \Sigma_t^{-1}(\delta)) dt + dM_t, \quad (3.9)$$

where  $M_t$  is defined as

$$dM_t := \left\langle \int_{\mathbb{R}^d} \|x - a_t\|_2^2 \Sigma_t^{-\frac{1}{2}}(\delta)(x - a_t) \mu_t(dx), dW_t \right\rangle,$$

which is a martingale started from zero with quadratic variation

$$d[M_t, M_t] = \left\| \int_{\mathbb{R}^d} \|x - a_t\|_2^2 \Sigma_t^{-\frac{1}{2}}(\delta)(x - a_t) \mu_t(dx) \right\|_2^2 dt. \quad (3.10)$$

Since  $\mu$  is log-concave, so is  $\mu_t$  (since  $p_t$  in (2.5) is log-concave). In particular, if  $x \sim \mu_t$ , then  $\Sigma_t^{-\frac{1}{2}}(x - a_t)$  follows a centered and isotropic log-concave distribution, which is denoted by  $\rho_t$ . Based on this observation, we can further bound (3.10) using the thin-shell constant  $\sigma_d^2$ :

$$\begin{aligned} & \left\| \int_{\mathbb{R}^d} \|x - a_t\|_2^2 \Sigma_t^{-\frac{1}{2}}(\delta)(x - a_t) \mu_t(dx) \right\|_2^2 \\ & \leq \int_{\mathbb{R}^d} \|x - a_t\|_2^4 \mu_t(dx) \int_{\mathbb{R}^d} \|\Sigma_t^{-\frac{1}{2}}(\delta)(x - a_t)\|_2^2 \mu_t(dx) && \text{(Cauchy-Schwarz)} \\ & = \int_{\mathbb{R}^d} |x^\top \Sigma_t x|^2 \rho_t(dx) \int_{\mathbb{R}^d} \|\Sigma_t^{-\frac{1}{2}}(\delta) \Sigma_t^{\frac{1}{2}} x\|_2^2 \rho_t(dx) && (x \leftarrow \Sigma_t^{-\frac{1}{2}}(x - a_t)) \\ & \leq \|\Sigma_t\|_2^2 \int_{\mathbb{R}^d} \|x\|_2^4 \rho_t(dx) \cdot d && \text{(Cauchy-Schwarz and } \mathbb{E}_{\rho_t}[\|x\|_2^2] = d) \\ & = d(d^2 + \text{Var}_{\rho_t}[\|x\|_2^2]) \|\Sigma_t\|_2^2 && \text{(Bias-variance decomposition)} \\ & \leq d^2(\sigma_d^2 + d) \|\Sigma_t\|_2^2, \end{aligned}$$

where

$$\sigma_d^2 := \sup_{\nu: \text{isotropic and log-concave on } \mathbb{R}^d} \frac{\text{Var}_{\nu}[\|x\|_2^2]}{d} \lesssim (\log d)^{4.5},$$

and the upper bound is due to [JLV22, Theorem 2]. Substituting these estimates back into (3.10) yields

$$d[M_t, M_t] \leq c_0 \|\Sigma_t\|_2^2 dt, \quad (3.11)$$

where  $c_0 > 0$  is some constant depending only on  $d$  (i.e.,  $c_0 \lesssim d^3$  but this may not be optimal).

We now apply Itô's formula to obtain the SDE for  $\log \text{tr}(\Sigma_t)$  using (3.9) and (3.11):

$$\begin{aligned} d \log \text{tr}(\Sigma_t) &= -\frac{\text{tr}(\Sigma_t^2 \Sigma_t^{-1}(\delta))}{\text{tr}(\Sigma_t)} dt + \frac{1}{\text{tr}(\Sigma_t)} dM_t - \frac{1}{2 \text{tr}(\Sigma_t)^2} d[M_t, M_t] \\ &\geq -\left(1 + \frac{c_0}{2}\right) dt + d\widetilde{M}_t, \end{aligned}$$

where  $d\widetilde{M}_t = \frac{1}{\text{tr}(\Sigma_t)} dM_t$  is another martingale started from zero with quadratic variation bounded by

$$d[\widetilde{M}_t, \widetilde{M}_t] = \frac{1}{\text{tr}(\Sigma_t)^2} d[M_t, M_t] \leq \frac{c_0 \|\Sigma_t\|_2^2}{\text{tr}(\Sigma_t)^2} dt \leq c_0 dt. \quad (3.12)$$

If we introduce the process  $X_t = \log \text{tr}(\Sigma_0) - \left(1 + \frac{c_0}{2}\right)t + \widetilde{M}_t$ , then  $\log \text{tr}(\Sigma_t) \geq X_t$ . Consequently, letting  $\tau' = \min\{s : X_s = \log(d\delta)\}$ , it follows that  $\tau' \leq \tau$ , so that  $\mathbb{P}(\tau \geq t) \geq \mathbb{P}(\tau' \geq t)$ .

To further lower bound  $\mathbb{P}(\tau' \geq t)$ , we use a time-changing argument. Applying the Dambis–Dubins–Schwarz theorem, we can represent  $X_t$  as a time-changed Brownian motion  $B_t$  with a constant drift:

$$X_t = -\left(1 + \frac{c_0}{2}\right)t + B_{[\widetilde{M}_t, \widetilde{M}_t]}.$$

Setting  $T = \frac{\log(\frac{1}{d\delta})}{2(2+c_0)}$  and denoting the cumulative distribution function of a standard normal by  $\Phi(x)$ ,

$$\begin{aligned} \mathbb{P}(\tau \geq T) &\geq \mathbb{P}(\tau' \geq T) = \mathbb{P}\left(\min_{0 \leq s \leq T} X_s \geq \log(d\delta)\right) \\ &\geq \mathbb{P}\left(\min_{0 \leq s \leq c_0 T} B_s \geq \frac{3}{4} \log(d\delta) - \log \text{tr}(\Sigma_0)\right) && ((3.12) + \text{choice of } T) \\ &= \mathbb{P}\left(\max_{0 \leq s \leq c_0 T} B_s \leq \frac{3}{4} \log\left(\frac{1}{d\delta}\right) + \log \text{tr}(\Sigma_0)\right) \\ &\geq \mathbb{P}\left(\max_{0 \leq s \leq c_0 T} B_s \leq \frac{1}{4} \log\left(\frac{1}{d\delta}\right)\right) && (d\delta < \text{tr}(\Sigma_0)^2) \\ &= \Phi\left(\frac{\log(\frac{1}{d\delta})}{4\sqrt{c_0 T}}\right) - \Phi\left(-\frac{\log(\frac{1}{d\delta})}{4\sqrt{c_0 T}}\right) && (\text{Reflection principle}) \\ &> \frac{3}{10}. && (d\delta < \frac{1}{4} + \text{choice of } T) \end{aligned}$$

This completes the proof.  $\square$

## 4 Joint stochastic localization

SL has been recognized as a novel sampling method to draw a sample from a target distribution. A less-explored application of SL is the construction of couplings. The first SL-based coupling construction appeared in the stability analysis of the Brunn–Minkowski inequality [Eld13, Section 5]. While that application was mainly intended to advance theory, it can be further developed into an algorithm to construct couplings between distributions.

Conceptually, the SL scheme in (2.1) can be extended to the setting of multiple distributions driven by the same Brownian motion. The control process  $C_t$  is used to tune the correlation of these distributions during the time evolution. For instance, consider two probability measures  $\mu$  and  $\nu$ , each associated with an SL scheme as follows:

$$\begin{aligned} dp_t(x) &= p_t(x) \langle x - a_t, C_t dW_t \rangle & a_t &= \int_{\mathbb{R}^d} x p_t(x) \mu(dx) \\ dq_t(x) &= q_t(x) \langle x - b_t, D_t dW_t \rangle & b_t &= \int_{\mathbb{R}^d} x q_t(x) \nu(dx) \end{aligned} \quad (4.1)$$

where  $W_t$  is a Brownian motion shared by  $p_t$  and  $q_t$ , and  $C_t, D_t$  are matrix-valued control processes adapted to  $W_t$ . This yields a pathwise dependence structure between  $\mu_t$  and  $\nu_t$  for every fixed  $t$ . Assuming both  $\mu_t$  and  $\nu_t$  localize as  $t \rightarrow \infty$ , a coupling between  $\mu$  and  $\nu$  can be obtained as  $(\text{supp}(\mu_\infty), \text{supp}(\nu_\infty))$ ; see Figure 2 for an illustration. In the remainder of this paper, we will take different choices of  $C_t$  and  $D_t$  in various applications of interest.

It should be noted that the joint SL scheme in (4.1) is just one of many possible options for coupling. Other constructions, such as those based on path-reversed Brownian motions, have been employed in different contexts to prove sharp functional inequalities [CFM24]. However, it is not clear whether those constructions can be turned into practical algorithms, which is a major focus of this paper.

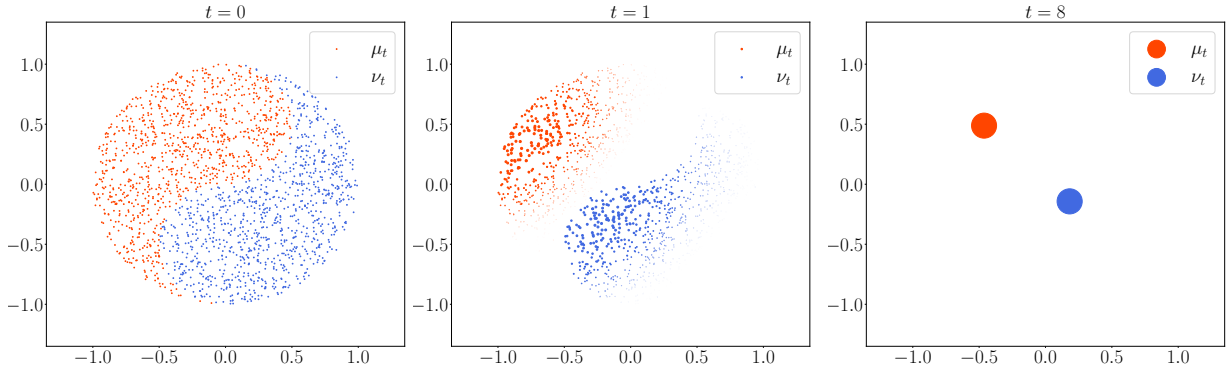


**Figure 2:** Joint SL of point cloud on the Yin and Yang Taichi logo using the (regularized) extrapolation scheme in (4.4). The initial distributions are uniform on the blue and red points, and time increases in the diagram as one goes from left to right. The size of the points is proportional to their weights.

As an initial application, we construct couplings between  $\mu$  and  $\nu$  with reduced transportation distance compared to the independence coupling. Among many possible choices, we choose one that extrapolates from known optimal transport solutions under certain scenarios. Recall that the  $p$ -Wasserstein distance ( $1 \leq p \leq \infty$ ) between  $\mu$  and  $\nu$  is defined as

$$W_p(\mu, \nu) = \min_{X \sim \mu, Y \sim \nu} \mathbb{E}[\|X - Y\|_p^p]^{\frac{1}{p}}, \quad (4.2)$$

where the minimum is taken over all couplings between  $\mu$  and  $\nu$ . Different choices of  $p$  induce different geometries in the probability space. In the following discussion, we take  $p = 2$ , as the cost function in this case is smooth, so we can leverage calculus tools facilitated by SL.

We now construct a joint SL scheme between  $\mu$  and  $\nu$  as follows:

$$\begin{aligned} dp_t(x) &= p_t(x) \langle x - a_t, C_t dW_t \rangle & a_t &= \int_{\mathbb{R}^d} x p_t(x) \mu(dx), \\ dq_t(x) &= q_t(x) \langle x - b_t, D_t dW_t \rangle & b_t &= \int_{\mathbb{R}^d} x q_t(x) \nu(dx), \end{aligned} \quad (4.3)$$

and  $\mu_t(dx) = p_t(x)\mu(dx)$  and  $\nu_t(dx) = q_t(x)\nu(dx)$ . Letting  $\Sigma_t$  and  $\Lambda_t$  denote covariances of  $\mu_t$  and  $\nu_t$ , respectively, i.e.,

$$\Sigma_t = \mathbb{E}_{\mu_t}[x \otimes x] - a_t \otimes a_t, \quad \Lambda_t = \mathbb{E}_{\nu_t}[x \otimes x] - b_t \otimes b_t,$$

the matrix-valued processes  $C_t$  and  $D_t$  are chosen as

$$C_t = (\Sigma_t^\dagger)^{\frac{1}{2}}, \quad D_t = \Sigma_t^{\frac{1}{2}} \left[ \left( \Sigma_t^{\frac{1}{2}} \Lambda_t \Sigma_t^{\frac{1}{2}} \right)^\dagger \right]^{\frac{1}{2}}. \quad (4.4)$$

The choice of  $C_t$  is the same as Eldan's  $\frac{1}{2}$ -scheme, while the choice of  $D_t$  depends on  $C_t$  and is inspired by the explicit optimal transport between normal distributions. In the rest of the paper, we call the joint SL scheme associated with (4.4) an *extrapolation scheme*, as it extrapolates the  $W_2$ -optimal couplings between normal distributions (Theorem 4.2).

At first sight, it is unclear whether  $\nu_t$  will eventually localize as  $t \rightarrow \infty$ . For instance, if  $\mu_t$  converges to a point mass at some finite time  $T$ , then  $\nu_t = \nu_T$  for all  $t \geq T$ , regardless of whether  $\nu_t$  is localized or not. In practice, this can be addressed by adding a small regularization term to  $\Sigma_t$  and  $\Lambda_t$  to enforce nondegeneracy. On the other hand, if both  $\mu$  and  $\nu$  are log-concave, then localization is ensured when  $t \rightarrow \infty$ .

**Theorem 4.1.** *If  $\mu$  and  $\nu$  are log-concave distributions in  $\mathbb{R}^d$ , then a.s., the extrapolation scheme defined in (4.3)-(4.4) exists for  $t > 0$  and localizes when  $t \rightarrow \infty$ .*

*Proof.* Since  $\mu_t$  is an Eldan's  $\frac{1}{2}$ -scheme, under the log-concavity assumption on  $\mu$ , both existence and localization for  $\mu_t$  follow from [Eld13, Lemma 2.4]. In particular,  $\Sigma_t$  is invertible for all  $t > 0$  a.s. Therefore,  $\nu_t$  follows an Eldan's  $\frac{1}{2}$ -scheme with Brownian motion  $W'_t$  where  $dW'_t = \Lambda_t^{\frac{1}{2}} \Sigma_t^{-\frac{1}{2}} (\Sigma_t^{-\frac{1}{2}} \Lambda_t^{-1} \Sigma_t^{-\frac{1}{2}})^{\frac{1}{2}} dW_t$  until  $\Lambda_t$  becomes singular. Since  $\nu$  is log-concave, a similar rescaling argument in the proof of [Eld13, Lemma 2.4] shows that this stopping time is infinity a.s. Hence,  $\nu_t$  follows an Eldan's  $\frac{1}{2}$ -scheme with Brownian motion  $W'_t$  for all  $t \geq 0$ , and the existence and localization results follow.  $\square$

Based on the joint SL scheme (4.3)-(4.4), we obtain a coupling between  $\mu$  and  $\nu$  with reduced mean Euclidean transportation distance compared to the independence coupling.

**Theorem 4.2.** *Let  $\mu$  and  $\nu$  be log-concave probability measures on  $\mathbb{R}^d$  with covariance matrices  $\Sigma_0$  and  $\Lambda_0$ , respectively. Then the extrapolation scheme defined in (4.3)-(4.4) converges to a joint point mass  $(a_\infty, b_\infty)$  as  $t \rightarrow \infty$ , which satisfies*

$$W_2^2(\mu, \nu) \leq \mathbb{E}[\|a_\infty - b_\infty\|_2^2] < \mathbb{E}[\|Z_\mu - Z_\nu\|_2^2], \quad (4.5)$$

where  $Z_\mu \sim \mu$  and  $Z_\nu \sim \nu$  are independent. If  $\mu$  is  $\kappa$ -strongly log-concave and  $\nu$  is Gaussian (i.e.,  $\mathcal{M}^{(3)}[\nu_t] = \int_{\mathbb{R}^d} (x - b_t)^{\otimes 3} \nu_t(dx) = 0$  for all  $t \geq 0$  since  $\nu_t$  remains Gaussian), then

$$W_2^2(\mu, \nu) \leq \mathbb{E}[\|a_\infty - b_\infty\|_2^2] < \|a_0 - b_0\|_2^2 + \text{tr}(\Sigma_0 + \Lambda_0) - 2\sqrt{\kappa \lambda_{\min}(\Lambda_0) \text{tr}(\Sigma_0)}, \quad (4.6)$$

where  $\lambda_{\min}(\Lambda_0)$  denotes the least eigenvalue of  $\Lambda_0$ . In the special case where both  $\mu$  and  $\nu$  are Gaussian,

$$W_2^2(\mu, \nu) = \mathbb{E}[\|a_\infty - b_\infty\|_2^2] = \|a_0 - b_0\|_2^2 + \text{tr}\left(\Sigma_0 + \Lambda_0 - 2(\Sigma_0^{\frac{1}{2}}\Lambda_0\Sigma_0^{\frac{1}{2}})^{\frac{1}{2}}\right). \quad (4.7)$$

**Remark 4.3.** We use  $(a_\infty, b_\infty)$  to denote the almost sure random limit of the posterior mean process  $(a_t, b_t)$ . The existence of the limit is implied by the localization result of Theorem 4.1. Moreover, this limit coincides with the support of  $(\mu_\infty, \nu_\infty)$ .

**Remark 4.4.** Applying (4.6) with  $\nu$  a centered Gaussian with covariance  $\frac{1}{\kappa}I$  (i.e.,  $\nu$  is  $\kappa$ -strongly log-concave), we obtain

$$W_2^2(\mu, \nu) \leq \|a_0 - b_0\|_2^2 + \text{tr}(\Sigma_0 + \Lambda_0) - 2\text{tr}(\Sigma_0) = \|a_0 - b_0\|_2^2 + \text{tr}(\Lambda_0) - \text{tr}(\Sigma_0).$$

Since  $\Lambda_0 \succeq \Sigma_0$  [EL14, Lemma 1], the right-hand side is nonnegative. This provides an upper bound on the  $W_2$ -distance between  $\kappa$ -strongly log-concave distributions and a normal distribution with covariance  $\frac{1}{\kappa}I$  via their mean and covariance matrices. In fact, (4.5)-(4.6) are not specific to the extrapolation scheme; for instance, taking  $C_t = (\Sigma_t^\dagger)^{\frac{1}{2}}$  and  $D_t = (\Lambda_t^\dagger)^{\frac{1}{2}}$  also works. This is called the joint Eldan's  $\frac{1}{2}$ -scheme, which is studied in detail in Section 5.1.

*Proof of Theorem 4.2.* For  $t \geq 0$ , applying (3.2) to both  $a_t$  and  $-b_t$  yields

$$d(a_t - b_t) = (\Sigma_t C_t - \Lambda_t D_t) dW_t. \quad (4.8)$$

By Itô's isometry,

$$\begin{aligned} \mathbb{E}[\|a_t - b_t\|_2^2] &= \|a_0 - b_0\|_2^2 + \int_0^t \text{tr}\left(\mathbb{E}[(\Sigma_s C_s - \Lambda_s D_s)(\Sigma_s C_s - \Lambda_s D_s)^\top]\right) ds \\ &= \|a_0 - b_0\|_2^2 + \int_0^t \text{tr}\left(\mathbb{E}[\Sigma_s + \Lambda_s - 2(\Sigma_s^{\frac{1}{2}}\Lambda_s\Sigma_s^{\frac{1}{2}})^{\frac{1}{2}}]\right) ds, \end{aligned} \quad (4.9)$$

where the second step follows from (4.4) and the cyclic property of the trace. Note that under the specific choice of  $C_t$  and  $D_t$  in (4.4),  $\mathbb{E}[\Sigma_t]$  and  $\mathbb{E}[\Lambda_t]$  are explicitly computable as  $\mathbb{E}[\Sigma_t] = \Sigma_0 e^{-t}$  and  $\mathbb{E}[\Lambda_t] = \Lambda_0 e^{-t}$  (since both  $\mu_t$  and  $\nu_t$  are Eldan's  $\frac{1}{2}$ -schemes but with different Brownian motions). Substituting these into (4.9) yields

$$\mathbb{E}[\|a_t - b_t\|_2^2] = \|a_0 - b_0\|_2^2 + (1 - e^{-t}) \text{tr}(\Sigma_0 + \Lambda_0) - 2 \int_0^t \text{tr}\left(\mathbb{E}[(\Sigma_s^{\frac{1}{2}}\Lambda_s\Sigma_s^{\frac{1}{2}})^{\frac{1}{2}}]\right) ds. \quad (4.10)$$

Taking  $t \rightarrow \infty$  and applying Fatou's lemma yields

$$\begin{aligned} \mathbb{E}[\|a_\infty - b_\infty\|_2^2] &= \mathbb{E}[\liminf_{t \rightarrow \infty} \|a_t - b_t\|_2^2] \\ &\leq \|a_0 - b_0\|_2^2 + \text{tr}(\Sigma_0 + \Lambda_0) - 2 \int_0^\infty \text{tr}\left(\mathbb{E}[(\Sigma_s^{\frac{1}{2}}\Lambda_s\Sigma_s^{\frac{1}{2}})^{\frac{1}{2}}]\right) ds \\ &= \mathbb{E}[\|Z_\mu - Z_\nu\|_2^2] - 2 \int_0^\infty \text{tr}\left(\mathbb{E}[(\Sigma_s^{\frac{1}{2}}\Lambda_s\Sigma_s^{\frac{1}{2}})^{\frac{1}{2}}]\right) ds \\ &< \mathbb{E}[\|Z_\mu - Z_\nu\|_2^2], \end{aligned}$$

where  $Z_\mu \sim \mu, Z_\nu \sim \nu$  are independent, and the last step used  $\int_0^t \text{tr} \left( \mathbb{E}[(\Sigma_s^{\frac{1}{2}} \Lambda_s \Sigma_s^{\frac{1}{2}})^{\frac{1}{2}}] \right) ds > 0$  by the path continuity of  $\Sigma_s$  and  $\Lambda_s$ .

Under the additional assumptions on  $\mu_t$  and  $\nu_t$ , we can quantify the above inequality by using the pathwise estimates for  $\|\Sigma_t\|_2$  [EL14, Lemma 2] and (3.4):  $\|\Sigma_t\|_2 \leq \frac{1}{\kappa} e^{-t}$  and  $\Lambda_t = \Lambda_0 e^{-t}$ . For the latter, the a.s.-vanishing of the third centered tensorial moment  $\mathcal{M}^{(3)}[\nu_t]$  makes  $\Lambda_t$  nonrandom under our choice of  $D_t$ :

$$d\Lambda_t = -\Lambda_t \Lambda_t^{\frac{1}{2}} \Sigma_t^{\frac{1}{2}} (\Sigma_t^{-\frac{1}{2}} \Lambda_t^{-1} \Sigma_t^{-\frac{1}{2}})^{\frac{1}{2}} (\Lambda_t^{\frac{1}{2}} \Sigma_t^{\frac{1}{2}} (\Sigma_t^{-\frac{1}{2}} \Lambda_t^{-1} \Sigma_t^{-\frac{1}{2}})^{\frac{1}{2}})^{\top} \Lambda_t dt = -\Lambda_t dt.$$

Consequently,

$$\begin{aligned} \int_0^\infty \text{tr} \left( \mathbb{E}[(\Sigma_s^{\frac{1}{2}} \Lambda_s \Sigma_s^{\frac{1}{2}})^{\frac{1}{2}}] \right) ds &\geq \sqrt{\lambda_{\min}(\Lambda_0)} \int_0^\infty e^{-\frac{s}{2}} \mathbb{E} \left[ \text{tr} \left( \Sigma_s^{\frac{1}{2}} \right) \right] ds \\ &\geq \sqrt{\kappa \lambda_{\min}(\Lambda_0)} \int_0^\infty \mathbb{E}[\text{tr}(\Sigma_s)] ds \\ &= \sqrt{\kappa \lambda_{\min}(\Lambda_0)} \text{tr}(\Sigma_0), \end{aligned}$$

where the second inequality follows from

$$\text{tr}(\Sigma_s) \leq \text{tr} \left( \Sigma_s^{\frac{1}{2}} \|\Sigma_s^{\frac{1}{2}}\|_2 \right) = \text{tr} \left( \Sigma_s^{\frac{1}{2}} \|\Sigma_s\|_2^{\frac{1}{2}} \right) \leq \frac{1}{\sqrt{\kappa}} e^{-\frac{s}{2}} \text{tr} \left( \Sigma_s^{\frac{1}{2}} \right).$$

Substituting this into (4.10) yields (4.6). When both  $\mu$  and  $\nu$  are Gaussian,  $\Sigma_t = \Sigma_0 e^{-t}$  and  $\Lambda_t = \Lambda_0 e^{-t}$ . This combined with (4.10) yields the second equality in (4.7). The first equality is well known [GS84, Proposition 7].  $\square$

## 5 Induced distances

### 5.1 Joint Eldan's $\alpha$ -scheme and induced distances

Although the extrapolation scheme in (4.4) extends the  $W_2$ -optimal couplings between normal distributions to log-concave distributions, the joint localization property may not hold beyond the log-concavity assumption. An alternative choice is to let  $C_t = (\Sigma_t^\dagger)^\alpha$  and  $D_t = (\Lambda_t^\dagger)^\alpha$ , a *joint Eldan's  $\alpha$ -scheme*.

The joint Eldan's  $\alpha$ -scheme is defined for all  $t \geq 0$  as long as the SL schemes associated with  $\mu$  and  $\nu$  are respectively defined. Under such circumstances, the posterior mean process  $(a_t, b_t)$  converges to some limit  $(a_\infty, b_\infty)$  as  $t \rightarrow \infty$  a.s., where  $(a_\infty, b_\infty)$  are joint random variables with  $a_\infty \sim \mu$  and  $b_\infty \sim \nu$ . This coupling can be consistently extended to any countable set of probability measures on  $\mathbb{R}^d$  as long as Eldan's  $\alpha$ -scheme is defined for each element in the set. The coupling between  $\mu$  and  $\nu$  through  $(a_\infty, b_\infty)$  induces a distance between  $\mu$  and  $\nu$  which is introduced next.

Fix  $\alpha \in [0, 1]$  and denote by  $\mathcal{P}_\alpha(\mathbb{R}^d)$  the set of probability measures on  $\mathbb{R}^d$  for which Eldan's  $\alpha$ -scheme is well-defined. As noted in Remark 3.2, probability measures with bounded support and smooth densities, or with finite support, belong to  $\mathcal{P}_\alpha(\mathbb{R}^d)$  for all  $\alpha \in [0, 1]$ . However, a sharp characterization of  $\mathcal{P}_\alpha(\mathbb{R}^d)$  is difficult unless  $\alpha = 0$ , which will be considered in Section 5.2.

**Definition 2** ( $\alpha$ -SL distance). Given  $\mu, \nu \in \mathcal{P}_\alpha(\mathbb{R}^d)$ , the  $\alpha$ -SL distance between  $\mu$  and  $\nu$  is defined by  $d_{\text{SL}_\alpha}(\mu, \nu) = \mathbb{E}[\|a_\infty - b_\infty\|_2^2]^{\frac{1}{2}}$ , where  $(a_\infty, b_\infty)$  is the limit of the posterior mean process  $(a_t, b_t)$  of a joint Eldan's  $\alpha$ -scheme associated with  $\mu$  and  $\nu$ .



By definition,  $d_{\text{SL}_\alpha}(\mu, \nu)$  measures the Euclidean transport cost between  $\mu$  and  $\nu$  under the particular coupling induced by joint Eldan's  $\alpha$ -scheme and is therefore lower bounded by  $W_2(\mu, \nu)$ . Other transport costs (e.g.,  $L^p$ -costs) may be considered, but we do not pursue this here.

The  $\alpha$ -SL distance satisfies a similar translation identity and invariance property under unitary transformations as  $W_2$ . When  $\alpha = \frac{1}{2}$ , an additional scaling property can be established. To derive these properties, we first state a lemma concerning the affine transformation of Eldan's  $\alpha$ -scheme.

**Lemma 1.** *Let  $\mu \in \mathcal{P}_\alpha(\mathbb{R}^d)$  and  $g(x) = Ax + c : \mathbb{R}^d \rightarrow \mathbb{R}^d$ , where  $A \in \mathbb{R}^{d \times d}$  is an invertible matrix and  $c \in \mathbb{R}^d$ . Denote by  $\mu_t$  an Eldan's  $\alpha$ -scheme associated with  $\mu$  with Brownian motion  $W_t$ . If we define  $\mu^g = g\#\mu$  and  $\mu_t^g = g\#\mu_t$  ( $\#$  denotes the pushforward measure), then  $\mu_t^g$  is an SL scheme with Brownian motion  $W_t$  and control process  $C_t = A^{-\top}[(A^{-1}\Sigma_t^g A^{-\top})^\dagger]^\alpha$ , where  $\Sigma_t^g$  is the covariance of  $\mu_t^g$ .*

*Proof.* Denote the density of  $\mu_t$  with respect to  $\mu$  as  $p_t$ . By the definition of pushforward measures,  $\mu_t^g \ll \mu^g$  with density  $p_t^g = p_t \circ g^{-1}$ , i.e.,  $p_t^g(x) = p_t(A^{-1}(x - c))$ . Moreover, the mean and covariance of  $\mu_t^g$ , denoted by  $a_t^g$  and  $\Sigma_t^g$ , are related to the mean and covariance of  $\mu_t$ , denoted by  $a_t$  and  $\Sigma_t$ , as follows:

$$a_t^g = Aa_t + c, \quad \Sigma_t^g = A\Sigma_t A^\top. \quad (5.1)$$

The desired result follows by noting that for every  $x \in \text{supp}(\mu^g)$ ,

$$\begin{aligned} dp_t^g(x) &= dp_t(A^{-1}(x - c)) \stackrel{(2.1)}{=} p_t(A^{-1}(x - c)) \left\langle A^{-1}(x - c) - a_t, (\Sigma_t^\dagger)^\alpha dW_t \right\rangle \\ &\stackrel{(5.1)}{=} p_t^g(x) \left\langle x - a_t^g, A^{-\top}[(A^{-1}\Sigma_t^g A^{-\top})^\dagger]^\alpha dW_t \right\rangle. \end{aligned}$$

□

Lemma 1 implies the following properties of the  $\alpha$ -SL distance.

**Theorem 5.1.** *Let  $\mu, \nu \in \mathcal{P}_\alpha(\mathbb{R}^d)$ .*

- (i) *(Translation identity) If  $\mu_{\text{cent}} = (I - \mathbb{E}_\mu[x])\#\mu$ ,  $\nu_{\text{cent}} = (I - \mathbb{E}_\nu[x])\#\nu$ , and  $c = \mathbb{E}_\mu[x] - \mathbb{E}_\nu[x]$ , then  $[d_{\text{SL}_\alpha}(\mu, \nu)]^2 = [d_{\text{SL}_\alpha}(\mu_{\text{cent}}, \nu_{\text{cent}})]^2 + \|c\|_2^2$ .*
- (ii) *(Unitary invariance) For any unitary matrix  $U \in \mathbb{R}^{d \times d}$ , if  $\mu^U = U\#\mu$  and  $\nu^U = U\#\nu$ , then  $d_{\text{SL}_\alpha}(\mu, \nu) = d_{\text{SL}_\alpha}(\mu^U, \nu^U)$ .*
- (iii) *(Homogeneity for  $\alpha = \frac{1}{2}$ ) Suppose  $\alpha = \frac{1}{2}$ . For any  $\gamma \in \mathbb{R}$ , if  $\mu^\gamma = (\gamma I)\#\mu$  and  $\nu^\gamma = (\gamma I)\#\nu$ , then  $d_{\text{SL}_\alpha}(\mu^\gamma, \nu^\gamma) = |\gamma|d_{\text{SL}_\alpha}(\mu, \nu)$ .*

**Remark 5.2.** An optimal coupling under  $W_2$  also satisfies the homogeneity property, i.e., if  $(X, Y)$  is a  $W_2$ -optimal coupling between  $\mu$  and  $\nu$ , then  $(\gamma X, \gamma Y)$  remains optimal under  $W_2$  for  $\mu^\gamma$  and  $\nu^\gamma$ . In this sense, the  $\frac{1}{2}$ -SL distance resembles the  $W_2$ -distance. Nonetheless, the desirability of homogeneity in practical applications remains debatable, especially in high-dimensional settings. Widely used statistical divergences, such as the KL divergence and the Fisher divergence, do not satisfy the homogeneity property. Interestingly, as we will see in Section 6, these divergences are closely related to the weighted 0-SL distance (Definition 3).

*Proof of Theorem 5.1.* We begin by introducing some notations. Let  $(\mu_t, \nu_t)$  be a joint Eldan's  $\alpha$ -scheme associated with  $\mu$  and  $\nu$  driven by Brownian motion  $W_t$ . The corresponding density process is denoted by  $(p_t, q_t)$ , the posterior mean process by  $(a_t, b_t)$ , and the covariance processes by  $(\Sigma_t, \Lambda_t)$ . By definition,  $(a_\infty, b_\infty) = \lim_{t \rightarrow \infty} (a_t, b_t)$  exists a.s. and provides a coupling defining  $d_{\text{SL}_\alpha}(\mu, \nu)$ .

For (i), note that by the bias-variance decomposition,

$$[d_{\text{SL}_\alpha}(\mu, \nu)]^2 = \mathbb{E}[\|a_\infty - b_\infty\|_2^2] = \mathbb{E}[\|(a_\infty - \mathbb{E}_\mu[x]) - (b_\infty - \mathbb{E}_\nu[x])\|_2^2] + \|c\|_2^2.$$

Since  $a_t - \mathbb{E}_\mu[x] = \mathbb{E}_{g\#\mu_t}[x]$  and  $b_t - \mathbb{E}_\nu[x] = \mathbb{E}_{h\#\nu_t}[x]$ , where  $g = I - \mathbb{E}_\mu[x]$  and  $h = I - \mathbb{E}_\nu[x]$ , it suffices to show that  $(g\#\mu_t, h\#\nu_t)$  is a joint Eldan's  $\alpha$ -scheme associated with  $(\mu_{\text{cent}}, \nu_{\text{cent}})$ . This follows directly from Lemma 1.

For (ii), let  $\mu_t^U = U\#\mu_t$  and  $\nu_t^U = U\#\nu_t$ , with their mean and covariance processes denoted by  $(a_t^U, b_t^U)$  and  $(\Sigma_t^U, \Lambda_t^U)$ , respectively. Applying Lemma 1 with  $A = U$  and  $c = 0$  yields that  $(\mu_t^U, \nu_t^U)$  is a joint SL scheme associated with  $(\mu^U, \nu^U)$  with Brownian motion  $W_t$  and control processes  $[(\Sigma_t^U)^\dagger]^\alpha U$  and  $[(\Lambda_t^U)^\dagger]^\alpha U$ . Alternatively,  $(\mu_t^U, \nu_t^U)$  is a joint Eldan's  $\alpha$ -scheme with Brownian motion  $W'_t = UW_t$ . Consequently, by the bounded convergence theorem,

$$\begin{aligned} [d_{\text{SL}_\alpha}(\mu, \nu)]^2 &= \lim_{t \rightarrow \infty} \mathbb{E}[\|a_t - b_t\|_\infty^2] = \lim_{t \rightarrow \infty} \mathbb{E}[\|Ua_t - Ub_t\|_\infty^2] \\ &= \lim_{t \rightarrow \infty} \mathbb{E}[\|a_t^U - b_t^U\|_\infty^2] = [d_{\text{SL}_\alpha}(\mu^U, \nu^U)]^2. \end{aligned} \quad (5.2)$$

The proof of (iii) is similar to (ii). Let  $\mu_t^\gamma = (\gamma I)\#\mu_t$  and  $\nu_t^\gamma = (\gamma I)\#\nu_t$ , with their mean and covariance processes denoted by  $(a_t^\gamma, b_t^\gamma)$  and  $(\Sigma_t^\gamma, \Lambda_t^\gamma)$ , respectively. Applying Lemma 1 with  $A = \gamma I$  and  $c = 0$  yields that  $(\mu_t^\gamma, \nu_t^\gamma)$  is a joint SL scheme associated with  $(\mu^\gamma, \nu^\gamma)$  with Brownian motion  $W_t$  and control processes  $\gamma^{2\alpha-1}[(\Sigma_t^\gamma)^\dagger]^\alpha$  and  $\gamma^{2\alpha-1}[(\Lambda_t^\gamma)^\dagger]^\alpha$ , which is a joint Eldan's  $\alpha$ -scheme if  $\alpha = \frac{1}{2}$ . The rest of the proof is similar to (5.2).  $\square$

More generally, we define the following extension of  $d_{\text{SL}_\alpha}$  to account for the dynamics in time when realizing the coupling through joint SL.

**Definition 3** (Weighted  $\alpha$ -SL distance). Let  $w$  be a probability measure on  $[0, \infty)$  with unbounded support. For  $\mu, \nu \in \mathcal{P}_\alpha(\mathbb{R}^d)$ , the  $w$ -weighted  $\alpha$ -SL distance between  $\mu$  and  $\nu$  is defined as

$$d_{\text{SL}_\alpha}^w(\mu, \nu) = \left( \int_0^\infty \mathbb{E}[\|a_t - b_t\|_2^2] w(dt) \right)^{\frac{1}{2}}, \quad (5.3)$$

where  $(a_t, b_t)$  is the posterior mean process of the joint Eldan's  $\alpha$ -scheme associated with  $\mu$  and  $\nu$ .

The  $\alpha$ -SL distance  $d_{\text{SL}_\alpha}(\mu, \nu)$  can be formally viewed as a special case of  $d_{\text{SL}_\alpha}^w(\mu, \nu)$  with  $w = \delta_\infty$ . The next Lemma shows that (5.3) is a well-defined distance function on  $\mathcal{P}_\alpha(\mathbb{R}^d)$ .

**Lemma 2.** *The  $w$ -weighted  $\alpha$ -SL distance in (5.3) is a well-defined distance function on  $\mathcal{P}_\alpha(\mathbb{R}^d)$ .*

*Proof.* By definition,  $d_{\text{SL}_\alpha}^w(\mu, \nu)$  is nonnegative, symmetric, and satisfies the triangle inequality. It remains to verify that for  $\mu, \nu \in \mathcal{P}_\alpha(\mathbb{R}^d)$ ,  $d_{\text{SL}_\alpha}^w(\mu, \nu) = 0$  if and only if  $\mu = \nu$ . The “if” direction is trivial by definition. For the “only if” direction, note that if  $\mu \neq \nu$ , then  $W_2(\mu, \nu) > 0$ , i.e., there exists  $\varepsilon > 0$  such that  $\mathbb{P}(\|a_\infty - b_\infty\|_2 > \varepsilon) > \varepsilon$ . Since  $(a_t, b_t) \rightarrow (a_\infty, b_\infty)$  a.s., they also converge

in probability:  $\mathbb{P}(\|a_t - a_\infty\|_2 > \frac{\varepsilon}{3}) \rightarrow 0$  and  $\mathbb{P}(\|b_t - b_\infty\|_2 > \frac{\varepsilon}{3}) \rightarrow 0$  as  $t \rightarrow \infty$ . Consequently, there exists a large  $T$  so that for all  $t \geq T$ ,  $\mathbb{P}(\|a_t - b_t\|_2 \geq \frac{\varepsilon}{3}) \geq \frac{\varepsilon}{3}$ . The desired result follows from the fact that  $w$  has unbounded support:

$$[\mathbf{d}_{\text{SL}_\alpha}^w(\mu, \nu)]^2 \geq \int_T^\infty \mathbb{E}[\|a_t - b_t\|_2^2] w(\mathrm{d}t) \geq \frac{\varepsilon^3}{27} w(\{t : t \geq T\}) > 0.$$

□

**Remark 5.3.** When  $\mu, \nu$  have bounded support,  $a_t - b_t$  is a martingale, so  $\|a_t - b_t\|_2^2$  is a submartingale, and thus  $\mathbb{E}[\|a_t - b_t\|_2^2]$  is nondecreasing in  $t$ . Consequently,

$$\sup_{w: |\text{supp}(w)|=\infty} \mathbf{d}_{\text{SL}_\alpha}^w(\mu, \nu) = \mathbf{d}_{\text{SL}_\alpha}(\mu, \nu).$$

Hence, both  $W_2(\mu, \nu)$  and  $\mathbf{d}_{\text{SL}_\alpha}^w(\mu, \nu)$  are bounded by  $\mathbf{d}_{\text{SL}_\alpha}(\mu, \nu)$ .

## 5.2 Topological equivalence between $\mathbf{d}_{\text{SL}_0}$ and $W_2$

To further understand  $\mathbf{d}_{\text{SL}_\alpha}$ , we focus on the scenario  $\alpha = 0$ . This specialization has two reasons. Conceptually, while different values of  $\alpha$  may induce different topologies, numerical simulation in Section 8 empirically suggests that  $\alpha = 0$  gives the “least-coupled” marginals when  $\alpha \leq \frac{1}{2}$  thus inducing the “finest” topology. Technically, setting  $\alpha = 0$  yields a constant control process which makes theoretical analysis tractable. Moreover,  $\mathcal{P}_0(\mathbb{R}^d)$  is sufficiently rich and contains all probability measures on  $\mathbb{R}^d$  with finite first moments. The next theorem shows that  $\mathbf{d}_{\text{SL}_0}$  is topologically equivalent to  $W_2$  for probability measures supported on a common compact set in  $\mathbb{R}^d$ .

**Theorem 5.4.** *The topologies induced by  $\mathbf{d}_{\text{SL}_0}$  and  $W_2$  are equivalent for probability measures supported on a common compact set in  $\mathbb{R}^d$ .*

*Proof.* Let  $\nu$  and  $\{\nu^{(n)}\}_n$  be probability measures with uniformly bounded support, i.e.,  $\text{supp}(\nu) \cup (\cup_{n=1}^\infty \text{supp}(\nu^{(n)})) \subset \Omega$  for some compact set  $\Omega \subset \mathbb{R}^d$ . It suffices to show that  $W_2(\nu, \nu^{(n)}) \rightarrow 0$  as  $n \rightarrow \infty$  if and only if  $\mathbf{d}_{\text{SL}_0}(\nu, \nu^{(n)}) \rightarrow 0$  as  $n \rightarrow \infty$ . The “if” direction is trivial since  $W_2$  is bounded by  $\mathbf{d}_{\text{SL}_0}$ . It remains to establish the “only if” direction.

Let  $(a_t, b_t)$  and  $(\theta_t, \theta'_t)$  denote the posterior mean process and observation process of the joint Eldan’s 0-scheme associated with  $\nu$  and  $\nu^{(n)}$ , respectively. In this case, one can use (2.5) to explicitly write  $a_t$  and  $b_t$  as a function of  $t$  and  $(\theta_t, \theta'_t)$ :

$$a_t = a_t(\theta_t) = \frac{\int_{\mathbb{R}^d} x h_t(x; \theta_t) \nu(\mathrm{d}x)}{\int_{\mathbb{R}^d} h_t(z; \theta_t) \nu(\mathrm{d}z)}, \quad b_t = b_t(\theta'_t) = \frac{\int_{\mathbb{R}^d} x h_t(x; \theta'_t) \nu^{(n)}(\mathrm{d}x)}{\int_{\mathbb{R}^d} h_t(z; \theta'_t) \nu^{(n)}(\mathrm{d}z)}, \quad (5.4)$$

where  $h_t(x; \theta) = \exp\{\langle x, \theta \rangle - \frac{t}{2} \|x\|_2^2\}$ . According to (2.6), one can write  $\theta_t$  and  $\theta'_t$  as

$$\theta_t = \int_0^t a_s \mathrm{d}s + W_t \quad \theta'_t = \int_0^t b_s \mathrm{d}s + W_t, \quad (5.5)$$

where  $W_t$  is the Brownian motion used in defining the joint Eldan’s 0-scheme associated with  $\nu$  and  $\nu^{(n)}$ .

By the localization property, we denote the a.s.-limit of  $(a_t, b_t)$  when  $t \rightarrow \infty$  as  $(a_\infty, b_\infty)$ . The path-continuity of  $(a_t, b_t)$  combined with (5.5) implies  $(a_\infty, b_\infty) = \lim_{t \rightarrow \infty} (\bar{\theta}_t, \bar{\theta}'_t)$  a.s., where  $(\bar{\theta}_t, \bar{\theta}'_t) := \frac{1}{t}(\theta_t, \theta'_t)$ . Combining this with Fatou's lemma gives

$$\begin{aligned} \mathbb{E}[\|a_\infty - b_\infty - (\bar{\theta}_t - \bar{\theta}'_t)\|_2^2] &\leq 2(\mathbb{E}[\|a_\infty - \bar{\theta}_t\|_2^2] + \mathbb{E}[\|b_\infty - \bar{\theta}'_t\|_2^2]) \\ &\leq \lim_{s \rightarrow \infty} 2(\mathbb{E}[\|\bar{\theta}_s - \bar{\theta}_t\|_2^2] + \mathbb{E}[\|\bar{\theta}'_s - \bar{\theta}'_t\|_2^2]). \end{aligned}$$

By the law-equivalent form of  $\theta_t$  in (2.7), we have  $\theta_t \equiv tX + W_t$  for  $X \sim \nu$  independent of  $W_t$ , from which it follows that

$$\lim_{s \rightarrow \infty} \mathbb{E}[\|\bar{\theta}_s - \bar{\theta}_t\|_2^2] = \lim_{s \rightarrow \infty} t \left( \frac{1}{t} - \frac{1}{s} \right)^2 + \frac{s-t}{s^2} = \frac{1}{t}.$$

Similarly,  $\lim_{s \rightarrow \infty} \mathbb{E}[\|\bar{\theta}'_s - \bar{\theta}'_t\|_2^2] = \frac{1}{t}$ . Consequently, we obtain

$$\mathbb{E}[\|a_\infty - b_\infty - (\bar{\theta}_t - \bar{\theta}'_t)\|_2^2] \leq \frac{4}{t}.$$

Since the convergence rate here is independent of  $n$ , given  $\varepsilon > 0$ , there exists  $T(\varepsilon) > 0$  (e.g.,  $T(\varepsilon) = \frac{4}{\varepsilon}$ ) such that for all  $n \geq 1$ ,

$$\mathbb{E}[\|a_\infty - b_\infty - (\bar{\theta}_t - \bar{\theta}'_t)\|_2^2] \leq \varepsilon \quad \text{for all } t \geq T. \quad (5.6)$$

Therefore, to bound  $\mathbb{E}[\|a_\infty - b_\infty\|_2^2]$ , it suffices to bound  $\mathbb{E}[\|\bar{\theta}_T - \bar{\theta}'_T\|_2^2]$  at finite time  $T$ , which can be achieved by a stability analysis of the SDEs in (5.5).

To this end, we first apply the Cauchy–Schwarz inequality to obtain the following estimate on  $\|\theta_t - \theta'_t\|_2^2$ :

$$\begin{aligned} \|\theta_t - \theta'_t\|_2^2 &\stackrel{(5.4)+(5.5)}{=} \left\| \int_0^t a_s(\theta_s) - b_s(\theta'_s) \, ds \right\|_2^2 \\ &\leq 2 \left\| \int_0^t a_s(\theta_s) - b_s(\theta_s) \, ds \right\|_2^2 + 2 \left\| \int_0^t b_s(\theta_s) - b_s(\theta'_s) \, ds \right\|_2^2 \\ &\leq 2t \underbrace{\int_0^t \|a_s(\theta_s) - b_s(\theta_s)\|_2^2 \, ds}_{(i)} + \underbrace{2 \int_0^t \|b_s(\theta_s) - b_s(\theta'_s)\|_2^2 \, ds}_{(ii)}. \end{aligned} \quad (5.7)$$

Terms (i) and (ii) can be further bounded as follows. To bound (i), we have

$$\begin{aligned} (i) &\stackrel{(5.4)}{=} \left\| \frac{\int_{\mathbb{R}^d} x h_s(x; \theta_s) \nu(dx)}{\int_{\mathbb{R}^d} h_s(z; \theta_s) \nu(dz)} - \frac{\int_{\mathbb{R}^d} x h_s(x; \theta_s) \nu^{(n)}(dx)}{\int_{\mathbb{R}^d} h_s(z; \theta_s) \nu^{(n)}(dz)} \right\|_2^2 \\ &\leq 2 \underbrace{\left\| \frac{\int_{\mathbb{R}^d} x h_s(x; \theta_s) \nu(dx)}{\int_{\mathbb{R}^d} h_s(z; \theta_s) \nu^{(n)}(dz)} - \frac{\int_{\mathbb{R}^d} x h_s(x; \theta_s) \nu^{(n)}(dx)}{\int_{\mathbb{R}^d} h_s(z; \theta_s) \nu^{(n)}(dz)} \right\|_2^2}_{(i.a)} + 2 \underbrace{\left\| \frac{\int_{\mathbb{R}^d} x h_s(x; \theta_s) \nu(dx)}{\int_{\mathbb{R}^d} h_s(z; \theta_s) \nu(dz)} - \frac{\int_{\mathbb{R}^d} x h_s(x; \theta_s) \nu^{(n)}(dx)}{\int_{\mathbb{R}^d} h_s(z; \theta_s) \nu^{(n)}(dz)} \right\|_2^2}_{(i.b)}. \end{aligned}$$

Since  $\Omega$  is compact, for every fixed  $\theta$ , denote the maximum of the Lipschitz constants of  $\frac{h_s(x; \theta)}{\int_{\mathbb{R}^d} h_s(z; \theta) \nu^{(n)}(dz)}$  and  $\frac{x_j h_s(x; \theta)}{\int_{\mathbb{R}^d} h_s(z; \theta) \nu^{(n)}(dz)}$  ( $j \leq d$ ) on  $\Omega$  by  $\text{Lip}_\Omega(\theta, \nu^{(n)})$ . Term (i.a) can be bounded using the Kantorovich–Rubinstein duality and Jensen's inequality:

$$(i.a) \leq d \text{Lip}_\Omega^2(\theta_s, \nu^{(n)}) W_1^2(\nu, \nu^{(n)}) \leq d \text{Lip}_\Omega^2(\theta_s, \nu^{(n)}) W_2^2(\nu, \nu^{(n)}).$$

Term (i.b) can be bounded by a similar reasoning:

$$\begin{aligned}
\text{(i.b)} &= \left| \frac{\int_{\mathbb{R}^d} h_s(x; \theta_s) \nu^{(n)}(dx)}{\int_{\mathbb{R}^d} h_s(z; \theta_s) \nu^{(n)}(dz)} - \frac{\int_{\mathbb{R}^d} h_s(x; \theta_s) \nu(dx)}{\int_{\mathbb{R}^d} h_s(z; \theta_s) \nu^{(n)}(dz)} \right|^2 \left\| \frac{\int_{\mathbb{R}^d} x h_s(x; \theta_s) \nu(dx)}{\int_{\mathbb{R}^d} h_s(z; \theta_s) \nu^{(n)}(dz)} \right\|_2^2 \\
&\leq \text{Lip}_\Omega^2(\theta_s, \nu^{(n)}) W_2^2(\nu, \nu^{(n)}) \|a_s\|_2^2 \\
&\leq \text{Lip}_\Omega^2(\theta_s, \nu^{(n)}) W_2^2(\nu, \nu^{(n)}) \text{diam}(\Omega)^2.
\end{aligned}$$

Combining the estimates on (i.a) and (i.b) yields the following upper bound on (i):

$$(i) \leq 2(d + \text{diam}(\Omega)^2) \text{Lip}_\Omega^2(\theta_s, \nu^{(n)}) W_2^2(\nu, \nu^{(n)}) \leq c_0 e^{c_0(1 + \|\theta_s\|_2 + s)} W_2^2(\nu, \nu^{(n)}), \quad (5.8)$$

where the last step follows from the fact that  $\sup_n \text{Lip}_\Omega^2(\theta_s, \nu^{(n)}) \leq \frac{c_0}{2(d + \text{diam}(\Omega)^2)} e^{c_0(1 + \|\theta_s\|_2 + s)}$  for some  $c_0 > 0$  depending only on  $\Omega$  and  $d$  (i.e., the denominator is not absorbed into  $c_0$  for convenience).

For (ii), we compute the Jacobian of  $b_s$  with respect to  $\theta$  as

$$\begin{aligned}
D_\theta b_s(\theta) &\stackrel{(5.4)}{=} D_\theta \left( \frac{\int_{\mathbb{R}^d} x h_s(x; \theta) \nu^{(n)}(dx)}{\int_{\mathbb{R}^d} h_s(z; \theta) \nu^{(n)}(dz)} \right) \\
&= \frac{\int_{\mathbb{R}^d} x \otimes x h_s(x; \theta) \nu^{(n)}(dx)}{\int_{\mathbb{R}^d} h_s(z; \theta) \nu^{(n)}(dz)} - \left( \frac{\int_{\mathbb{R}^d} x h_s(x; \theta) \nu^{(n)}(dx)}{\int_{\mathbb{R}^d} h_s(z; \theta) \nu^{(n)}(dz)} \right)^{\otimes 2},
\end{aligned}$$

which is the covariance of  $\xi$  for  $\xi(dx) \propto h_s(x; \theta) \nu^{(n)}(dx)$ . Since  $\text{supp}(\nu^{(n)}) \subset \Omega$  for all  $n$ ,  $\sup_\theta \|D_\theta b_s(\theta)\|_2^2 \leq \text{diam}(\Omega)^2$ . Consequently,

$$\|b_s(\theta_s) - b_s(\theta'_s)\|_2^2 \leq \text{diam}(\Omega)^2 \|\theta_s - \theta'_s\|_2^2. \quad (5.9)$$

Substituting (5.8)-(5.9) into (5.7) and taking expectation both sides,

$$\begin{aligned}
\mathbb{E}[\|\theta_t - \theta'_t\|_2^2] &\leq 2c_0 T W_2^2(\nu, \nu^{(n)}) \int_0^T \mathbb{E}[e^{c_0(1 + \|\theta_s\|_2 + s)}] ds + 2\text{diam}(\Omega)^2 T \int_0^t \mathbb{E}[\|\theta_s - \theta'_s\|_2^2] ds \\
&\leq c_1 W_2^2(\nu, \nu^{(n)}) + c_1 \int_0^t \mathbb{E}[\|\theta_s - \theta'_s\|_2^2] ds,
\end{aligned}$$

where the second inequality follows from (2.7) (which implies  $\|\theta_s\|_2 \leq t \text{diam}(\Omega) + \|W_t\|_2$ ) and  $c_1(c_0, T, \text{diam}(\Omega)) > 0$  depends on  $c_0$ ,  $T$ , and  $\text{diam}(\Omega)$ . Applying Grönwall's inequality, there exists a constant  $c_2(c_1) > 0$  (independent of  $n$ ) such that

$$\mathbb{E}[\|\bar{\theta}_T - \bar{\theta}'_T\|_2^2] \leq \frac{1}{T^2} \mathbb{E}[\|\theta_T - \theta'_T\|_2^2] \leq \frac{c_2 W_2^2(\nu, \nu^{(n)}) e^{c_2 T}}{T^2}.$$

Since  $W_2(\nu, \nu^{(n)}) \rightarrow 0$  as  $n \rightarrow \infty$ , there exists some  $N > 0$  such that for all  $n \geq N$ ,  $\mathbb{E}[\|\bar{\theta}_T - \bar{\theta}'_T\|_2^2] \leq \varepsilon$ . This combined with (5.6) yields  $d_{\text{SL}_0}(\nu, \nu^{(n)}) = \mathbb{E}[\|a_\infty - b_\infty\|_2^2] \leq 4\varepsilon$  for all  $n \geq N$ . The proof is concluded by noting that  $\varepsilon$  is arbitrary.  $\square$

## 6 Connections to statistical divergences

We give some connections between  $d_{\text{SL}_0}^w$  and statistical divergences, including the Gaussian KL divergence and a weighted Fisher divergence in the context of training diffusion models. Although our results in this section are established by leveraging existing observations plus a change-of-variable argument, they shed light on the geometry captured by  $d_{\text{SL}_0}$ . In the rest of this section, we often use  $B_t$  to denote a Brownian motion to distinguish from the Brownian motion  $W_t$  used in defining joint SL schemes.

### 6.1 Connection to the Gaussian KL divergence

It is well known that Eldan's 0-scheme is closely related to Föllmer processes [Föl88], which exhibit certain entropy-minimization properties when transporting the Wiener measure to other measures defined on Wiener space. Following this observation, under an appropriate choice of  $w$ , we connect  $d_{\text{SL}_0}^w$  to an approximate form of the Gaussian KL divergence.

Let  $B_t$  be a Brownian motion in  $\mathbb{R}^d$  and  $\nu$  be the Gaussian measure on  $\mathbb{R}^d$  (i.e.,  $B_1 \sim \nu$ ). For any  $\mu \ll \nu$  with  $\frac{d\mu}{d\nu} = f$ , the Föllmer drift  $v_t(x)$  associated with  $\mu$  is defined as the solution to the following optimal control problem:

$$\min_v \frac{1}{2} \int_0^1 \mathbb{E}[\|v_t(X_t)\|_2^2] dt \quad \text{where } dX_t = v_t(X_t) dt + dB_t \text{ satisfies } X_1 \sim \mu. \quad (6.1)$$

Under mild regularity conditions on  $\mu$ , the Föllmer drift is unique and admits an explicit form:  $v_t(x) = \nabla \log P_{1-t}f(x)$ , where  $P_t$  is the heat semigroup with  $P_t f(x) = \mathbb{E}[f(x + B_t)]$  [Leh13]. The process  $X_t$  driven by the Föllmer drift is called the Föllmer process associated with  $\mu$ . As such, we may consider the embedding  $\mathcal{E}$  that maps  $\mu$  to the path measure of its Föllmer process. The inverse of  $\mathcal{E}$  is called the Brownian transport map, which provides a unified approach to studying functional inequalities [MS24].

The objective in (6.1) is the transport cost associated with the Cameron–Martin norm [FÜ04]. By Girsanov's theorem, it is also equal to the KL divergence between the path measure of  $\{X_t\}_{0 \leq t \leq 1}$  and the Wiener measure on  $C([0, 1], \mathbb{R}^d)$ :

$$\frac{1}{2} \int_0^1 \mathbb{E}[\|v_t(X_t)\|_2^2] dt = \text{KL}(\mathcal{E}(\mu) \|\mathcal{E}(\nu)) = \text{KL}(\mu \|\nu), \quad (6.2)$$

where the second equality is known and follows from the fact that  $\frac{d\mathcal{E}(\mu)}{d\mathcal{E}(\nu)}(\omega)$  depends only on the terminal value of  $\omega$  at  $t = 1$ . A useful connection between Eldan's 0-scheme and the Föllmer process is as follows.

**Lemma 3** ([KP23]). *Let  $\theta_t$  be the observation process of Eldan's 0-scheme associated with  $\mu$  as defined in (2.8), and  $X_t$  be the Föllmer process associated with  $\mu$ . Then,  $\{X_t\}_{0 \leq t \leq 1} = \{(1-t)\theta_{\zeta(t)}\}_{0 \leq t \leq 1}$ , where  $\zeta(t) = \frac{t}{1-t}$  for  $t \in [0, 1]$  and equality is in law.*

Lemma 3 implies the following representation of  $\text{KL}(\mu \|\nu)$  using the posterior mean process of the joint Eldan's 0-scheme associated with  $\mu$  and  $\nu$ .

**Theorem 6.1.** *Let  $\nu$  be the Gaussian measure on  $\mathbb{R}^d$  and assume that  $\mu \ll \nu$  has a unique Föllmer process. Let  $(a_t, b_t)$  be the posterior mean process of the joint Eldan's 0-scheme associated with  $\mu$  and  $\nu$ . The KL divergence between  $\mu$  and  $\nu$  can be represented as follows:*

$$\text{KL}(\mu \|\nu) = \frac{1}{2} \int_0^\infty \mathbb{E} \left[ \left\| (1+t)(a_t - b_t) - \int_0^t (a_s - b_s) ds \right\|_2^2 \right] w(dt), \quad (6.3)$$

where the weight measure  $w$  is defined as  $w(dt) = \frac{1}{(1+t)^2} \mathbb{I}_{\{t \geq 0\}} dt$ .

**Remark 6.2.** Formula (6.3) does not fit into the definition of  $d_{\text{SL}_0}^w$ . However, if we replace  $\int_0^t (a_s - b_s) ds$  by  $t(a_t - b_t)$ , which serves as an effective approximation for large  $t$ , then (6.3) becomes  $\frac{1}{2} d_{\text{SL}_0}^w$  with the same  $w$  in Theorem 6.1. This suggests that  $d_{\text{SL}_0}^w$  can be viewed as an analogue of the Gaussian KL divergence, though  $d_{\text{SL}_0}^w$  is a valid distance that does not require additional assumptions on  $\mu$  and  $\nu$  beyond bounded second moments.

*Proof of Theorem 6.1.* Denote  $X_t$  and  $Y_t$  as the Föllmer processes associated with  $\mu$  and  $\nu$ , respectively. Let  $(\theta_t, \theta'_t)$  be the observation process of a joint Eldan's 0-scheme associated with  $\mu$  and  $\nu$  with Brownian motion  $W_t$ . By Lemma 3 and the definition of  $(\theta_t, \theta'_t)$ ,  $X_t$  and  $Y_t$  satisfy the following SDEs:

$$\begin{aligned} dX_t &= d(1-t)\theta_{\zeta(t)} = \left( \frac{a_{\zeta(t)}}{1-t} - \theta_{\zeta(t)} \right) dt + (1-t) dW_{\zeta(t)} = \left( \frac{a_{\zeta(t)}}{1-t} - \theta_{\zeta(t)} \right) dt + dB_t, \\ dY_t &= \left( \frac{b_{\zeta(t)}}{1-t} - \theta'_{\zeta(t)} \right) dt + dB_t, \end{aligned}$$

where  $dB_t = (1-t) dW_{\zeta(t)}$  is a Brownian motion (which can be checked using Lévy's characterization of Brownian motion). Under the uniqueness assumption on the solution to the Föllmer process, we have

$$\begin{aligned} \text{KL}(\mu \parallel \nu) &\stackrel{(6.2)}{=} \frac{1}{2} \int_0^1 \mathbb{E} \left[ \left\| \frac{a_{\zeta(t)}}{1-t} - \theta_{\zeta(t)} - \frac{b_{\zeta(t)}}{1-t} + \theta'_{\zeta(t)} \right\|_2^2 \right] dt \quad \left( \frac{b_{\zeta(t)}}{1-t} - \theta'_{\zeta(t)} = 0 \right) \\ &= \frac{1}{2} \int_0^\infty \mathbb{E} \left[ \left\| (1+t)(a_t - b_t) - \int_0^t (a_s - b_s) ds \right\|_2^2 \right] w(dt) \quad (t \leftarrow \zeta(t) + \text{definition of } w), \end{aligned}$$

proving the desired result.  $\square$

## 6.2 Connection to the score-matching objectives

We next establish a connection between  $d_{\text{SL}_0}$  and the score-matching objectives used in training diffusion models [Son+20]. Diffusion models are a type of generative models that estimate a target distribution through two stochastic processes: a forward process transforming data into noise and a backward process converting a noisy sample into data that mimics the target distribution. These two processes are time reversals of each other, with the backward process typically approximated by a hypothesis class (e.g., neural networks) and serving as the engine for new data generation. See [TZ24] for a mathematical overview of the related topics.

To illustrate a connection between score-matching and  $d_{\text{SL}_0}^w$ , let  $B_t$  be a Brownian motion in  $\mathbb{R}^d$  and consider a diffusion model with an Ornstein–Uhlenbeck (OU) forward process  $X_t$ :

$$dX_t = -X_t dt + \sqrt{2} dB_t, \quad X_0 \sim \mu. \quad (6.4)$$

The initial distribution  $\mu$  is the target of learning and assumed to have bounded second moment.

Now fix  $T > 0$  and consider the time-reversal of  $X_t$  over  $[0, T]$  defined by  $Y_t = X_{T-t}$  for  $0 \leq t \leq T$ , which is a time-inhomogeneous Markov process with its law described by the following SDE [And82]:

$$dY_t = (Y_t + 2\nabla \log p_{T-t}(Y_t)) dt + \sqrt{2} dB_t, \quad Y_0 \sim X_T, \quad (6.5)$$



where  $p_{T-t}$  denotes the density of  $X_{T-t}$  and depends on  $\mu$ . Here we have slightly abused the notation  $B_t$  as they have different sample paths in (6.4) and (6.5). The main idea of diffusion models is that one can generate an exact sample of  $\mu$  by running the backward process (6.5) up to time  $T$ , which is, however, a nontrivial task. Fortunately, due to the fast mixing property of the OU process, the starting point  $Y_0 = X_T$  is approximately normally distributed when  $T$  is moderately large, regardless of  $\mu$ . The remaining challenge, therefore, lies in simulating the drift in (6.5). In particular, the term  $\nabla \log p_t(x)$ , known as Stein's score function of  $X_t$ , depends on  $\mu$  and thus is unavailable in practice.

A common approach to addressing this issue is to approximate  $\nabla \log p_t(x)$  using the score-matching mechanism, which can be formulated as the following problem:

$$\min_{\vartheta \in \Theta} \int_0^T \lambda(t) \mathbb{E}_{x \sim X_t} [\|\nabla \log p_t(x) - s_t(x; \vartheta)\|_2^2] dt, \quad (6.6)$$

where  $\lambda(t) : [0, T] \rightarrow \mathbb{R}_+$  is some positive weight function and  $\{s_t(x; \vartheta) : \mathbb{R}^d \rightarrow \mathbb{R}^d \mid \vartheta \in \Theta \subseteq \mathbb{R}^r\}$  represents the hypothesis class for approximation. This minimization problem can be equivalently converted to a computationally feasible form via integration by parts [HD05]:

$$\min_{\vartheta \in \Theta} \int_0^T \lambda(t) \mathbb{E}_{(x_0, x) \sim (X_0, X_t)} [\|\nabla \log p_t(x|x_0) - s_t(x; \vartheta)\|_2^2] dt, \quad (6.7)$$

where  $p_t(x|x_0)$  is the transition kernel from  $X_0$  to  $X_t$  and is known explicitly. In particular, problem (6.7) can be numerically solved using empirical minimization based on the samples of  $X_0$ . For theoretical analysis, however, we directly work with (6.6).

Under the choice of the forward process in (6.4), for fixed  $t$ ,  $X_t = e^{-t}X_0 + \sqrt{1 - e^{-2t}}W$ , where  $W \sim N(0, I)$  is independent of  $X_0$  and equality is in law. As a result,  $\nabla \log p_t(x)$  can be written in terms of the posterior mean function  $\mathbb{E}[X_0|X_t = x]$  via Tweedie's formula [Rob92]:

$$\nabla \log p_t(x) = \frac{e^t \mathbb{E}[X_0|X_t = x]}{e^{2t} - 1} - \frac{e^{2t}x}{e^{2t} - 1}. \quad (6.8)$$

To relate the objective in (6.6) to  $d_{\text{SL}_0}^w$ , we need an additional assumption on the hypothesis class. For  $s(x; \vartheta)$  in an arbitrary hypothesis class, its associated backward process (i.e., (6.5) with the drift replaced by  $Y_t + 2s(Y_t; \vartheta)$ ) may not correspond to the time-reversal of an OU process. In other words, given  $\vartheta$ , there may not exist a probability measure  $\nu$  such that  $Z_t$  defined by  $dZ_t = s_t(Z_t; \vartheta) dt + \sqrt{2} dB_t$  coincides in law with the time-reversal of an OU process (6.4) started from  $\nu$ . Alternatively, one can directly approximate  $\mu$  by  $\nu(\cdot; \vartheta)$  (assumed to have bounded second moment). By virtue of (6.8), this induces a parametrization on scores as

$$s_t(x; \vartheta) = \frac{e^t \mathbb{E}[Z_0^\vartheta|Z_t^\vartheta = x]}{e^{2t} - 1} - \frac{e^{2t}x}{e^{2t} - 1}, \quad (6.9)$$

where  $Z_t^\vartheta$  is an OU process started from  $\nu(\cdot; \vartheta)$ . With this parametrization, we can rewrite (6.6) as the following minimization problem:

$$\min_{\vartheta \in \Theta} \int_0^T \frac{e^{2t} \lambda(t)}{(e^{2t} - 1)^2} \mathbb{E}_{x \sim X_t} [\|\mathbb{E}[X_0|X_t = x] - \mathbb{E}[Z_0^\vartheta|Z_t^\vartheta = x]\|_2^2] dt. \quad (6.10)$$

The next lemma, which shares a similar spirit to Lemma 3, will be needed for our observation in Theorem 6.3. Let  $\theta_t$  be the observation process of Eldan's 0-scheme associated with  $\mu$ .

**Lemma 4** ([Mon23]). Let  $\tau(t) = \frac{1}{e^{2t}-1}$ . If we define the time-changed reversal of  $X_t$  as  $\bar{Y}_t = X_{\tau(t)}$ , then  $\{\theta_t\}_t = \{\sqrt{t(1+t)}\bar{Y}_t\}_t$ , where equality is in law.

We are now ready to state our main observation.

**Theorem 6.3.** If the drift in (6.5) is parametrized through  $\nu(\cdot, \vartheta)$  as in (6.9), then the minimization problem in (6.10) is equivalent to the following minimization problem:

$$\min_{\vartheta \in \Theta} \int_0^\infty \mathbb{E}_{x \sim \theta_t} [\|a_t(x) - b_t(x; \vartheta)\|_2^2] w(dt), \quad (6.11)$$

where  $(a_t, b_t) = (a_t(\theta_t), b_t(\theta'_t; \vartheta))$  is the posterior mean process of joint Eldan's 0-scheme associated with  $\mu$  and  $\nu(\cdot; \vartheta)$  with  $(\theta_t, \theta'_t)$  being the corresponding observation process, and  $w(dt) = \frac{1}{2} \lambda(\tau(t)) \tau'(\tau(t)) \tau'(t) \mathbb{I}_{\{t \geq \tau^{-1}(T)\}} dt$  is a  $\sigma$ -finite measure with support  $[\tau^{-1}(T), \infty)$  for the same  $\tau(t)$  in Lemma 4.

**Remark 6.4.** When  $w$  is a finite measure, i.e.,

$$w(\mathbb{R}) = \frac{1}{2} \int_{\tau^{-1}(T)}^\infty \lambda(\tau(t)) \tau'(\tau(t)) \tau'(t) dt = \int_0^T \frac{e^{2t} \lambda(t)}{(e^{2t} - 1)^2} dt < \infty, \quad (6.12)$$

$w$  can be normalized to a probability measure on  $\mathbb{R}_+$  with unbounded support, and this will not affect the optimization problem. In this case, we may assume  $w(\mathbb{R}) = 1$  and compare the objective in (6.11) with  $d_{\text{SL}_0}^w$  with the same  $w$ :

$$d_{\text{SL}_0}^w(\mu, \nu) = \int_0^\infty \mathbb{E}_{(x, x') \sim (\theta_t, \theta'_t)} [\|a_t(x) - b_t(x'; \vartheta)\|_2^2] w(dt).$$

Hence,  $d_{\text{SL}_0}^w$  can be seen as an analogue of the score-matching loss, but it compares the posterior mean functions on coupled trajectories of  $\theta_t$  and  $\theta'_t$  rather than on a single trajectory of  $\theta_t$ . This, in some sense, suggests that  $d_{\text{SL}_0}^w$  is more stringent than the score-matching objectives.

To get additional evidence on the heuristics, assume that  $\lambda(t)$  is uniformly bounded on  $[0, T]$ . Under such circumstances, the integrability condition (6.12) is equivalent to  $\int_0^T t^{-2} \lambda(t) dt < \infty$  since  $\frac{e^{2t}}{(e^{2t}-1)^2} \sim \frac{1}{4t^2}$  as  $t \rightarrow 0$ . For instance, taking  $\lambda(t) \propto t^{1+\varepsilon}$  would work for any  $\varepsilon > 0$ . On the other hand, a popular choice of  $\lambda(t)$  used in practice [Son+20, Section 3.3] sets

$$\lambda(t) \propto \frac{1}{\mathbb{E}_{(x_0, x_t) \sim (X_0, X_t)} [\|\nabla \log p_t(x|x_0)\|_2^2]} = \frac{1 - e^{-2t}}{d} \sim \frac{2t}{d} \quad \text{as } t \rightarrow 0,$$

where  $p_t(x|x_0)$  is the transition kernel from  $X_0$  to  $X_t$ . This choice, however, yields  $w(\mathbb{R}) = \infty$ . Consequently, the corresponding  $d_{\text{SL}_0}^w$  becomes trivial since  $d_{\text{SL}_0}^w(\mu, \nu) = \infty$  if  $\mu \neq \nu$ .

*Proof of Theorem 6.3.* Let  $\xi(t) = \sqrt{t(1+t)}$  for  $t \in [0, \infty]$ . Fixing  $t > 0$ , we apply Lemma 4 to conclude that, a.s.,

$$\begin{aligned} \mathbb{E}[X_0 | X_t = x] &\stackrel{(i)}{=} \lim_{\varepsilon \rightarrow 0} \mathbb{E}[X_\varepsilon | X_t = x] \\ &= \lim_{\varepsilon \rightarrow 0} \frac{1}{\xi(\tau^{-1}(\varepsilon))} \mathbb{E}[\theta_{\tau^{-1}(\varepsilon)} | \theta_{\tau^{-1}(t)} = \xi(\tau^{-1}(t))x] \quad (\text{Lemma 4}) \\ &\stackrel{(ii)}{=} \lim_{\varepsilon \rightarrow 0} \mathbb{E} \left[ \frac{\tau^{-1}(\varepsilon)}{\xi(\tau^{-1}(\varepsilon))} X_0 + \frac{W_{\tau^{-1}(\varepsilon)}}{\xi(\tau^{-1}(\varepsilon))} \mid \theta_{\tau^{-1}(t)} = \xi(\tau^{-1}(t))x \right] \\ &\stackrel{(iii)}{=} \mathbb{E}[X_0 \mid \theta_{\tau^{-1}(t)} = \xi(\tau^{-1}(t))x] \\ &\stackrel{(iv)}{=} a_{\tau^{-1}(t)}(\xi(\tau^{-1}(t))x), \end{aligned}$$

where (i) follows from the path-continuity of  $X_t$  and the dominated convergence theorem applied to  $\sup_{0 \leq t \leq 1} \|X_t\|_2$ , (ii) follows from the law-equivalent representation of  $\theta_t$  in (2.7) with  $C_t = I$ , (iii) follows from the dominated convergence theorem, i.e.,

$$\sup_{\varepsilon \leq \tau(1)} \left\| \frac{\tau^{-1}(\varepsilon)}{\xi(\tau^{-1}(\varepsilon))} X_0 + \frac{W_{\tau^{-1}(\varepsilon)}}{\xi(\tau^{-1}(\varepsilon))} \right\|_2 \leq \|X_0\|_2 + \sup_{s \leq 1} s \|W_{1/s}\|_2$$

and the right-hand side is integrable since  $sW_{1/s}$  can be identified as a Brownian motion in  $\mathbb{R}^d$  by time inversion, and (iv) follows from Remark 2.1.

If  $Z_t^\vartheta$  is an OU process started from  $\nu(\cdot; \vartheta)$ , then by a similar reasoning,  $\mathbb{E}[Z_0^\vartheta | Z_t^\vartheta = x] = b_{\tau^{-1}(t)}(\xi(\tau^{-1}(t))x)$  a.s., where  $b_t(\theta_t; \vartheta)$  is the posterior mean process of Eldan's 0-scheme associated with  $\nu(\cdot; \vartheta)$ . Consequently, the proof is completed by noting

$$\begin{aligned} & \int_0^T \frac{e^{2t}\lambda(t)}{(e^{2t}-1)^2} \mathbb{E}_{x \sim X_t} \left[ \|\mathbb{E}[X_0 | X_t = x] - \mathbb{E}[Z_0^\vartheta | Z_t^\vartheta = x]\|_2^2 \right] dt \\ &= \int_0^T -\frac{\lambda(t)\tau'(t)}{2} \mathbb{E}_{x \sim X_t} \left[ \|a_{\tau^{-1}(t)}(\xi(\tau^{-1}(t))x) - b_{\tau^{-1}(t)}(\xi(\tau^{-1}(t))x; \vartheta)\|_2^2 \right] dt \quad (\tau'(t) = -\frac{2e^{2t}}{(e^{2t}-1)^2}) \\ &= \int_{\tau^{-1}(T)}^\infty \frac{\lambda(\tau(t))\tau'(\tau(t))\tau'(t)}{2} \mathbb{E}_{x \sim X_{\tau(t)}} \left[ \|a_t(\xi(t)x) - b_t(\xi(t)x; \vartheta)\|_2^2 \right] dt \quad (t \leftarrow \tau^{-1}(t)) \\ &= \int_0^\infty \mathbb{E}_{x \sim \theta_t} \left[ \|a_t(x) - b_t(x; \vartheta)\|_2^2 \right] w(dt). \quad (\text{Lemma 4} + \text{definition of } w) \end{aligned}$$

□

## 7 Distribution estimation

Motivated by the ideas in Section 6, we propose a parametric approach to approximate a target distribution  $\mu$ . We choose  $k \leq d$  as the dimension of some latent space of variables, a probability measure  $\gamma_k$  on  $\mathbb{R}^k$  that is easy to sample from (e.g., uniform measure on  $[0, 1]^k$  or the standard normal distribution), and a parametric family of deterministic mappings  $f_\vartheta := f(\cdot; \vartheta) : \mathbb{R}^k \rightarrow \mathbb{R}^d$ . The parameters  $\vartheta$  are assumed to belong to a set  $\Theta \subseteq \mathbb{R}^J$ . Our approximation of  $\mu$  is  $\tilde{\mu} = f_\vartheta \# \gamma_k$ , where  $\hat{\vartheta}$  is chosen as

$$\hat{\vartheta} = \arg \min_{\vartheta \in \Theta} [\text{d}_{\text{SL}_\alpha}(\mu, f_\vartheta \# \gamma_k)]^2. \quad (7.1)$$

Throughout we are assuming that  $\mu, f_\nu \# \gamma_k \in \mathcal{P}_\alpha(\mathbb{R}^d)$  for all  $\vartheta \in \Theta$ .

Since  $\text{d}_{\text{SL}_\alpha}$  is defined as an expectation over joint Eldan's  $\alpha$ -scheme, the objective function in (7.1) can be approximated via MC approximation:

$$[\text{d}_{\text{SL}_\alpha}(\mu, \nu)]^2 \approx \frac{1}{M} \sum_{j=1}^M \|a_\infty^{(j)} - b_\infty^{(j)}(\vartheta)\|_2^2,$$

where  $\{(a_t^{(j)}, b_t^{(j)}(\vartheta))_{0 \leq t \leq \infty}\}_{j=1}^M$  are  $M$  i.i.d. trajectories of the posterior mean process of joint Eldan's  $\alpha$ -scheme associated with  $\mu$  and  $\nu(\cdot; \vartheta)$ . The resulting empirical version of the minimization problem in (7.1) is

$$\min_{\vartheta \in \Theta} \frac{1}{M} \sum_{j=1}^M \|a_\infty^{(j)} - b_\infty^{(j)}(\vartheta)\|_2^2. \quad (7.2)$$

In practical scenarios,  $\mu$  is often approximated by the empirical measure over some training dataset  $\mathcal{X} = \{X_1, \dots, X_{N_1}\} \subset \mathbb{R}^d$ . To solve (7.1) numerically, we further approximate  $\gamma_k$  using a random/quasi-random sequence  $\mathcal{Z} = \{Z_1, \dots, Z_{N_2}\} \subset \mathbb{R}^k$ . With slight abuse of notation, we denote

$$\mu = \frac{1}{N_1} \sum_{i=1}^{N_1} \delta_{X_i}, \quad \nu(\cdot; \vartheta) = \frac{1}{N_2} \sum_{i=1}^{N_2} \delta_{f(Z_i; \vartheta)}. \quad (7.3)$$

In this case, the joint Eldan's  $\alpha$ -scheme associated with  $\mu$  and  $\nu(\cdot; \vartheta)$  is well-defined because both measures have finite support (Remark 3.2).

Under continuity assumptions, one can apply gradient-based methods to solve (7.2). To this end, we consider a joint Eldan's  $\alpha$ -scheme between  $\mu$  and  $\nu(\cdot; \vartheta)$ . The corresponding localization profile  $\nu_\infty(\vartheta)$ , which can be identified as  $(\nu_\infty(f(z_1; \vartheta)), \dots, \nu_\infty(f(z_{N_2}; \vartheta))) \in \{0, 1\}^{N_2}$  assuming  $f(z_i; \vartheta)$  are distinct, is a vector-valued random field indexed by  $\vartheta \in \Theta$  as ensured by the Kolmogorov extension theorem. Fixing  $\vartheta$ , if we denote the localization profile  $b_\infty^{(j)}(\vartheta)$  as  $\nu_\infty^{(j)}(\vartheta)$  and assume it is continuous at  $\vartheta$ , then  $D_\vartheta \nu_\infty^{(j)}(\vartheta) = \mathbf{0}$ , where  $D_\vartheta$  is the Jacobian with respect to  $\vartheta$ . In this case, the gradient of the  $j$ th summand with respect to  $\vartheta$  can be computed as follows:

$$\begin{aligned} \nabla_\vartheta \|a_\infty^{(j)} - b_\infty^{(j)}(\vartheta)\|_2^2 &= 2[D_\vartheta(b_\infty^{(j)}(\vartheta))]^\top (b_\infty^{(j)}(\vartheta) - a_\infty^{(j)}) \\ &= 2 \left[ D_\vartheta \left( \sum_{i=1}^{N_2} \nu_\infty^{(j)}(f(Z_i; \vartheta)) f(Z_i; \vartheta) \right) \right]^\top (b_\infty^{(j)}(\vartheta) - a_\infty^{(j)}) \\ &= 2 \left[ \sum_{i=1}^{N_2} \nabla_\vartheta \nu_\infty^{(j)}(f(Z_i; \vartheta)) f^\top(Z_i; \vartheta) + \nu_\infty^{(j)}(f(Z_i; \vartheta)) D_\vartheta f(Z_i, \vartheta) \right]^\top (b_\infty^{(j)}(\vartheta) - a_\infty^{(j)}) \\ &= 2 \left[ \sum_{i=1}^{N_2} \nu_\infty^{(j)}(f(Z_i; \vartheta)) D_\vartheta f(Z_i, \vartheta) \right]^\top (b_\infty^{(j)}(\vartheta) - a_\infty^{(j)}) \\ &= 2[D_\vartheta f(Z_{i_j}, \vartheta)]^\top (b_\infty^{(j)}(\vartheta) - a_\infty^{(j)}), \end{aligned} \quad (7.4)$$

where  $1 \leq i_j \leq N_2$  satisfies  $\nu_\infty^{(j)}(f(Z_{i_j}; \vartheta)) = 1$ . Based on this, one can further compute the Hessian as

$$\nabla_\vartheta^2 \|a_\infty^{(j)} - b_\infty^{(j)}(\vartheta)\|_2^2 = 2[D_\vartheta^2 f(Z_{i_j}, \vartheta)]^\top (b_\infty^{(j)}(\vartheta) - a_\infty^{(j)}) + 2[D_\vartheta f(Z_{i_j}, \vartheta)]^\top D_\vartheta f(Z_{i_j}, \vartheta). \quad (7.5)$$

Typically,  $a_\infty^{(j)}$  and  $b_\infty^{(j)}(\vartheta)$  cannot be evaluated exactly but are instead approximated by  $a_T^{(j)}$  and  $b_T^{(j)}(\vartheta)$  for some large  $T > 0$ . For  $0 < \alpha \leq \frac{1}{2}$ , if we discretize  $[0, T]$  into  $L$  subintervals, then evaluation of  $a_T^{(j)}$  and  $b_T^{(j)}(\vartheta)$  requires  $\mathcal{O}(L(d^3 + Nd^2))$  operations in total, where  $N = N_1 + N_2$ . This includes computing the control matrix, which has complexity  $\mathcal{O}(Nd^2 + d^3)$  per step, and updating  $p_t(x)$  for all  $x$ , which takes  $\mathcal{O}(Nd)$  per step. The overall complexity can be reduced to  $\mathcal{O}(LNd)$  if  $\alpha = 0$  (since simulating joint Eldan's 0-scheme does not require computing the control matrix), but the effective  $L$  can be much larger to get localization as a result of the relatively slow convergence rate of Eldan's 0-scheme.

## 8 Numerical simulation

This section provides numerical experiments to support our theoretical findings. We first simulate Eldan's  $\alpha$ -scheme with different values of  $\alpha$  to demonstrate the varying localization rates.

Next, we use their joint versions and the extrapolation scheme (4.4) to compute upper bounds on the  $W_2$ -distance between simulated distributions and to illustrate their induced coupling structures. Finally, we employ the proposed distribution estimation formulation (7.1) to approximate a target distribution. All experiments were conducted using Python on a MacBook Air (M4, 2025).

To simulate SL, we apply the Euler–Maruyama method to the log-density evolution in (2.4) with a uniform time step  $\Delta t = 0.05$ . The density is normalized at each step. When implementing Eldan’s  $\alpha$ -scheme, we regularize the corresponding control process as  $C_t = (\Sigma_t + \delta^{\frac{1}{\alpha}} I)^{-\alpha}$  for some  $\delta > 0$  to ensure a consistent level of numerical stability (i.e., this choice ensures that  $\|C_t\|_2 \leq \frac{1}{\delta}$  for all different values of  $\alpha$ ), instead of directly using  $C_t = (\Sigma_t^\dagger)^\alpha$ . This regularization is also applied in the extrapolation scheme when computing the pseudoinverse (which can be viewed as a variant of joint Eldan’s  $\frac{1}{2}$ -scheme). We choose  $\delta = 0.003$  in Section 8.1 and  $\delta = 0.001$  in Sections 8.2–8.3; the former choice is slightly larger to better illustrate the mixed effects of finite-time convergence and regularization when  $\alpha > \frac{1}{2}$ . In all examples, errors introduced by numerical discretization are not considered.

### 8.1 Localization rates of Eldan’s $\alpha$ -scheme

We apply Eldan’s  $\alpha$ -scheme to sample from two distributions in  $\mathbb{R}^2$ : a uniform distribution on a convex domain (log-concave) and a Gaussian mixture (multimodal). The distribution parameters are given below:

Case 1 :  $\text{Unif}([-1, 1]^2)$ ;

Case 2 :  $\frac{1}{2}N\left(\begin{bmatrix} 0 \\ 0 \end{bmatrix}, \begin{bmatrix} 0.1 & 0 \\ 0 & 0.1 \end{bmatrix}\right) + \frac{3}{10}N\left(\begin{bmatrix} 1 \\ 0 \end{bmatrix}, \begin{bmatrix} 0.1 & 0 \\ 0 & 0.1 \end{bmatrix}\right) + \frac{1}{5}N\left(\begin{bmatrix} 0 \\ 1 \end{bmatrix}, \begin{bmatrix} 0.1 & 0 \\ 0 & 0.1 \end{bmatrix}\right).$

The true distribution is discretized using an empirical measure over 500 i.i.d. samples. The values of  $\alpha$  are chosen from  $\{0, 0.3, 0.5, 0.8, 1\}$ , and the time horizon is set to  $T = 10$ . We simulate  $10^4$  trajectories of SL for each  $\alpha$  and use the same seeds across all  $\alpha$ . At each step, we compute the average trace of the covariance matrix  $\Sigma_t$  of the SL process  $\mu_t$  and plot its logarithm against time. The results are given in Figure 3.

As shown in Figure 3, the general trend of localization rates aligns with Theorem 3.1, with a larger value of  $\alpha$  indicating faster localization. In particular,  $\alpha = 0.5$  exhibits exponential convergence within the tested regime, as evidenced by the straight line in the plot, while  $\alpha > 0.5$  converges in finite time (i.e., it slows down after a certain threshold due to regularization).

### 8.2 Bounding the $W_2$ -distance

Couplings induced by joint SL schemes provide computable upper bounds on the  $W_2$ -distance. In this example, we apply joint Eldan’s  $\alpha$ -scheme with the same  $\alpha$  in Section 8.1 (i.e.,  $\alpha \in \{0, 0.3, 0.5, 0.8, 1\}$ ) and the extrapolation scheme (4.4) to numerically estimate (upper bounds on) the  $W_2$ -distance between simulated distributions. For the choice of distributions, we consider two types with different geometries: a Gaussian mixture and distributions supported on annuli.

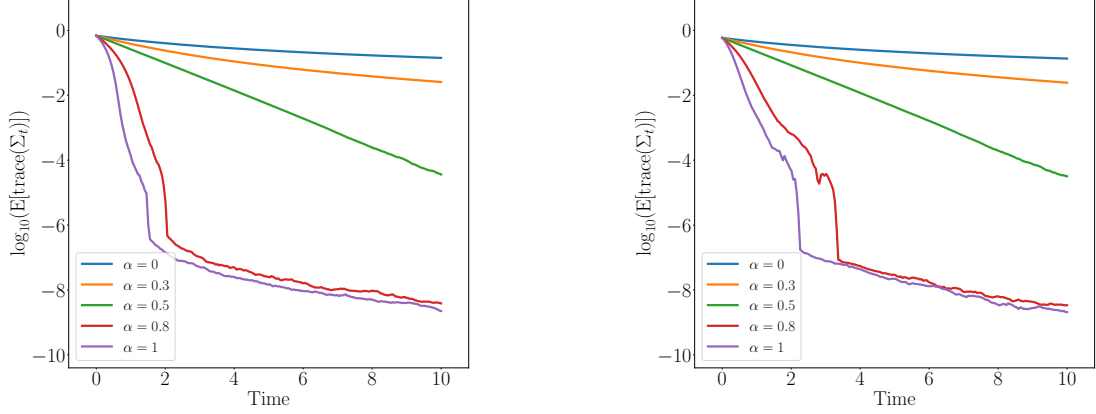


**Figure 3:** Localization rates of Eldan’s  $\alpha$ -scheme for two different distributions in  $\mathbb{R}^2$ : a uniform distribution over  $[-1, 1]^2$  (left) and a Gaussian mixture with three components (right).

The specific setups are given below:

$$\text{Case 1 : } \mu \sim \sum_{i=1}^4 \frac{1}{4} N \left( \begin{bmatrix} \frac{1}{\sqrt{2}} & -\frac{1}{\sqrt{2}} \\ \frac{1}{\sqrt{2}} & \frac{1}{\sqrt{2}} \end{bmatrix}^i \begin{bmatrix} 4 \\ 0 \end{bmatrix}, \begin{bmatrix} 0.1 & 0 \\ 0 & 0.1 \end{bmatrix} \right),$$

$$\nu \sim \sum_{i=1}^4 \frac{1}{4} N \left( \begin{bmatrix} \frac{1}{\sqrt{2}} & -\frac{1}{\sqrt{2}} \\ \frac{1}{\sqrt{2}} & \frac{1}{\sqrt{2}} \end{bmatrix}^i \begin{bmatrix} 2\sqrt{2} \\ 2\sqrt{2} \end{bmatrix}, \begin{bmatrix} 0.1 & 0 \\ 0 & 0.1 \end{bmatrix} \right);$$

$$\text{Case 2 : } \mu \sim \text{Unif}(\{x \in \mathbb{R}^2 : 1.5 \leq \|x\|_2 \leq 2\}),$$

$$\nu \sim \frac{1}{2} \text{Unif}(\{x \in \mathbb{R}^d : 0.5 \leq \|x\|_2 \leq 1\}) + \frac{1}{2} \text{Unif}(\{x \in \mathbb{R}^d : 0.2 \leq \|x + (0, 4)^\top\|_2 \leq 0.4\}).$$

We sample 200 i.i.d. points from  $\mu$  and  $\nu$  to represent their corresponding distributions. To simulate SL, we set  $T = 10^4$  to ensure that all schemes are sufficiently localized. We simulate  $10^3$  trajectories for each scheme and compute the mean-squared transportation distance by averaging. We also compute the 95% confidence interval (CI) based on the estimated variances. As a baseline, we calculate the mean-squared transportation distance under both the optimal and independence couplings. The joint samples obtained under Eldan’s  $\alpha$ -scheme with  $\alpha = 0, 0.5, 1$ , the extrapolation scheme, and the optimal coupling under  $W_2$ , are shown in Figure 4, while the estimated statistics are reported in the tables in Figure 5.

In both scenarios, all joint SL schemes encode nontrivial dependence structures between the marginals, as seen from the reduced mean transport cost compared to the independence coupling. In this regard, the extrapolation scheme yields the strongest dependence and mimics the optimal coupling. The joint Eldan’s  $\alpha$ -scheme exhibits similar performance as the extrapolation scheme when  $\alpha = 0.5$ , with the mean-squared transportation distance slightly increasing as  $\alpha \rightarrow 0$ . However, when  $\alpha \rightarrow 1$ , the mean-squared transportation distance increases dramatically, resulting in a degraded coupling. In particular, when  $\alpha = 1$ , the mean-squared transportation distance resembles that of the independence coupling (despite being different from it, since the independence coupling does not induce a distance).

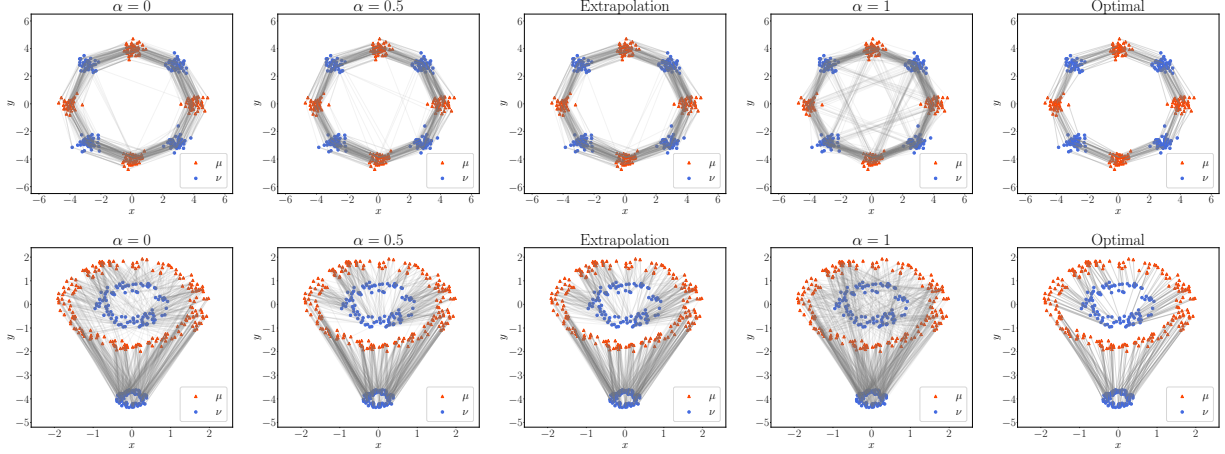


**Figure 4:** Simulated data from  $\mu$  and  $\nu$  in Case 1 (top) and Case 2 (bottom). A line connecting two points represents a joint sample obtained in the MC simulation of the corresponding joint SL schemes.

Coupling	Bound on $W_2$	95% CI	Coupling	Bound on $W_2$	95% CI
Joint Eldan's 0	2.99	[2.95, 3.02]	Joint Eldan's 0	2.53	[2.45, 2.60]
Joint Eldan's 0.3	2.92	[2.88, 2.96]	Joint Eldan's 0.3	2.40	[2.33, 2.46]
Joint Eldan's 0.5	2.87	[2.82, 2.91]	Joint Eldan's 0.5	2.39	[2.33, 2.45]
Joint Eldan's 0.8	3.29	[3.20, 3.38]	Joint Eldan's 0.8	2.78	[2.70, 2.86]
Joint Eldan's 1	3.74	[3.62, 3.86]	Joint Eldan's 1	3.08	[2.98, 3.17]
Extrapolation	2.84	[2.81, 2.87]	Extrapolation	2.38	[2.32, 2.44]
Optimal	2.61	NA	Optimal	2.28	NA
Independence	5.70	NA	Independence	3.31	NA

**Figure 5:** Estimated bounds on the  $W_2$ -distance using different joint SL schemes in Case 1 (left) and Case 2 (right). The 95% CI is also given based on the estimated variances.



### 8.3 Distribution estimation

We apply formulation (7.1) to estimate a distribution in  $\mathbb{R}^3$  supported on a 2D compact manifold. The target distribution  $\mu$  is taken as the pushforward measure of the uniform distribution on  $[-1, 1]^2$  (denoted by  $\gamma_2$ ) under the following map  $f : \mathbb{R}^2 \rightarrow \mathbb{R}^3$ :

$$f : \begin{bmatrix} x \\ y \end{bmatrix} \mapsto \begin{bmatrix} e^{0.5x+y} \\ -e^{x-0.5y} \\ x + 2y^2 \end{bmatrix}.$$

We generate  $N_1 = 1000$  i.i.d. samples from  $\mu$  and use them as training data. To approximate  $\mu$ , we parametrize  $f$  using multivariate polynomial regression:

$$f(x, y; \vartheta) = \begin{bmatrix} \sum_{0 \leq i, j \leq 2} \vartheta_{ij1} P_i(x) P_j(y) \\ \sum_{0 \leq i, j \leq 2} \vartheta_{ij2} P_i(x) P_j(y) \\ \sum_{0 \leq i, j \leq 2} \vartheta_{ij3} P_i(x) P_j(y) \end{bmatrix},$$

where  $P_i$  is the normalized univariate Legendre polynomial on  $[-1, 1]$  with degree  $i$ , and the coefficient vector  $\vartheta = (\vartheta_{ij\ell}) \in \mathbb{R}^{27}$ . Moreover, we discretize  $\gamma_2$  by an empirical distribution over an Sobol' sequence  $\{Z_i\}_{i=1}^{N_2}$  with length  $N_2 = 1024$  (rescaled to  $[-1, 1]^2$ ) and fix it throughout the experiment. The hypothesis class is given by

$$\left\{ \nu(x, y; \vartheta) = \frac{1}{N_2} \sum_{i=1}^{N_2} \delta_{f(Z_i; \vartheta)} \mid \vartheta \in \mathbb{R}^{27} \right\}.$$

To approximate  $\mu$ , we solve (7.2) with  $\alpha = 0.5$ . This choice of  $\alpha$  is mainly due to its fast localization rate. Moreover, we set  $M = 2000$  and the time horizon  $T = 10$ . For optimization, we employ the Newton conjugate gradient trust-region method with a maximum of 20 iterations (`scipy.optimize` [Vir+20]). Since the optimization is nonconvex, an informed initialization is chosen to help find a good local minimum. To this end, we choose  $\vartheta$  so that  $\nu(x, y; \vartheta)$  coincides with the shifted embedding of  $Z_i$  in  $\mathbb{R}^3$ , matched in mean to  $\mu$  and rotated to the subspace spanned by the first two principal components of  $\mu$ . For comparison, we also consider a (uninformed) random initialization  $\vartheta \sim N(0, 0.1I)$ . The corresponding results are given in Figure 6.

For both initializations, the convergence occurs within approximately 10 iterations. The resulting estimated distributions approximately recover the shape of  $\mu$ , although the estimation under uninformed initialization appears to be a local minimum (the optimality of the estimation in the informed case is difficult to check). These findings offer preliminary yet encouraging evidence for the effectiveness of  $\alpha$ -SL distances in distribution estimation. Nevertheless, solving the associated optimization problem can be computationally intensive when the dimension  $d$  is large. Moreover, the quality of the solution is sensitive to initialization. A potential practical remedy to address these challenges involves the use of randomized algorithms with batch-based updates (e.g., stochastic gradient descent), combined with expressive hypothesis classes such as neural networks. We leave these investigations for future work.

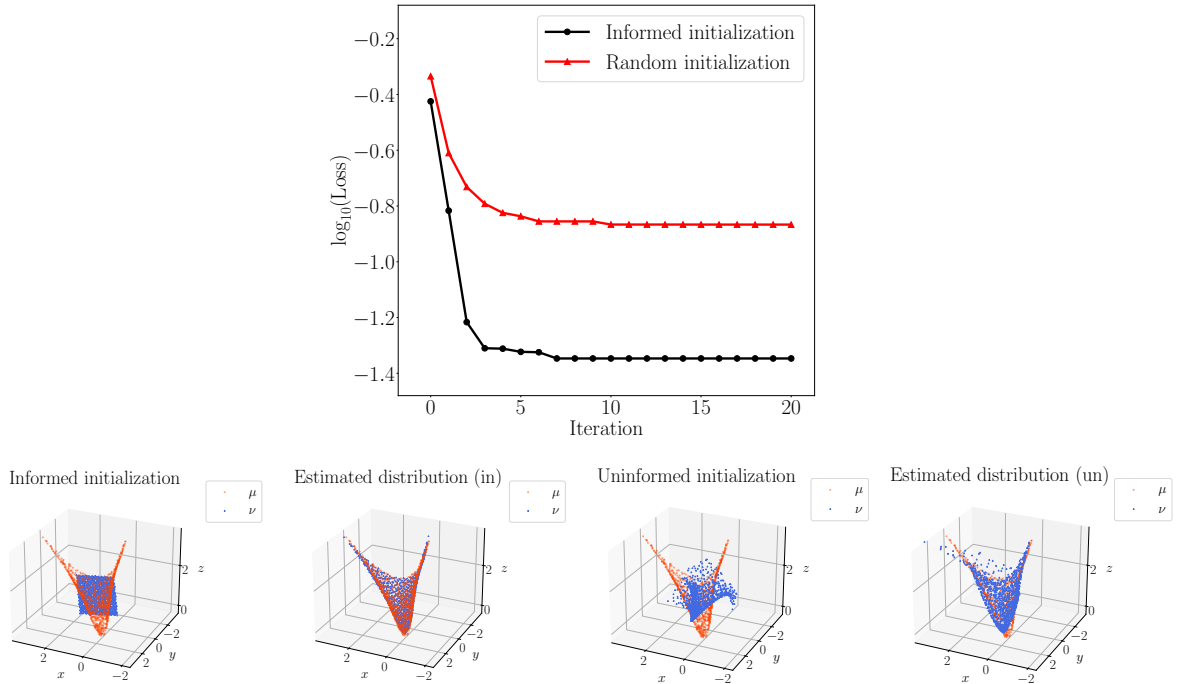


**Figure 6:** Loss decay (plotted in  $\log_{10}$ -scale against iterations) for both informed and uninformed initializations (top) and visualizations of the initializations along with their corresponding estimated distributions  $\nu$  (bottom).

## 9 Conclusion and future work

In this paper, we studied several algorithmic aspects of SL as a computational technique. This includes providing a unified perspective on various existing SL schemes, investigating their localization rates and regularization, and introducing a flexible joint SL framework for constructing couplings between probability distributions. We further demonstrated how to use the proposed framework to obtain approximate optimal transport between log-concave distributions, as well as to define a family of distributional distances. Owing to the algorithmic nature of SL, the proposed distances also inspire new approaches to distribution learning.

Since many results in this paper are conceptually nascent, they open up several directions for future investigation. For instance, a substantial part of this paper has focused on the analysis of  $d_{\text{SL}_0}$  due to its technical tractability. In particular, we showed that  $d_{\text{SL}_0}$  can be seen as a suitable analogue of various statistical divergences. On the other hand, in the case  $\alpha = \frac{1}{2}$ , although an exact analysis of  $d_{\text{SL}_\alpha}$  is quite difficult, the homogeneity property of  $d_{\text{SL}_\alpha}$  and associated coupling structures (which are empirical) suggest that it resembles the  $W_2$ -distance. This implies that  $d_{\text{SL}_\alpha}$ , as  $\alpha$  varies from 0 to  $\frac{1}{2}$ , interpolates between the entropy-based divergence and the transport-based distance. Further understanding of this phenomenon (either theoretical or numerical) is an interesting direction worth pursuing in the future.

On the computational side, this paper did not account for the approximation errors (including numerical errors resulting from discretization of SDEs and statistical errors resulting from MC simulation) when simulating SL or joint SL. Rigorously quantifying these errors is a necessary task. Moreover, when the dimension is high, simulation of Eldan’s  $\alpha$ -scheme is quite expensive when  $\alpha > 0$  as it requires the second-order statistics of the SL process. Incorporating randomization techniques to accelerate the numerical implementation may be necessary to ensure its

scalability to high-dimensional settings. We leave these questions for future investigation.

## Acknowledgment

Y. Xu would like to thank Dan Mikulincer for his kind explanation of some results in [EMZ20] and for his insightful suggestions, which inspired the discussion in Section 6.1. Y. Xu also thanks Joseph Lehec and Fei Pu for providing helpful references during the preparation of this paper. We would like to thank Xiyue Han for reading through Section 3 in the paper. T. Alberts is supported in part by the Simons Foundation Travel Support for Mathematicians grant MPS-TSM-00002584 and NSF grant DMS-2136198. Y. Xu is supported by start-up funding from the University of Kentucky and by the AMS-Simons Travel Grant 3048116562. Q. Ye is supported in part by the NSF under grants DMS-2208314, IIS-2327113, and ITE-2433190.

## References

- [And82] B. Anderson. “Reverse-time diffusion equation models”. *Stochastic Processes and their Applications* 12.3 (1982), pp. 313–326.
- [ACB17] M. Arjovsky, S. Chintala, and L. Bottou. “Wasserstein Generative Adversarial Networks”. In: *Proceedings of the 34th International Conference on Machine Learning*. Ed. by D. Precup and Y. W. Teh. Vol. 70. Proceedings of Machine Learning Research. PMLR, 2017, pp. 214–223.
- [BG21] E. Bayraktar and G. Guo. “Strong equivalence between metrics of Wasserstein type”. *Electronic Communications in Probability* 26 (2021).
- [Ben+23] J. Benton, V. De Bortoli, A. Doucet, and G. Deligiannidis. “Linear convergence bounds for diffusion models via stochastic localization”. *arXiv preprint arXiv:2308.03686* (2023).
- [Bon+15] N. Bonneel, J. Rabin, G. Peyré, and H. Pfister. “Sliced and radon wasserstein barycenters of measures”. *Journal of Mathematical Imaging and Vision* 51 (2015), pp. 22–45.
- [Bon13] N. Bonnotte. “Unidimensional and evolution methods for optimal transportation”. PhD thesis. Université Paris Sud-Paris XI; Scuola normale superiore (Pise, Italie), 2013.
- [Bou86a] J. Bourgain. “Geometry of Banach spaces and harmonic analysis”. In: *Proceedings of the International Congress of Mathematicians*. Vol. 1. Citeseer, 1986, p. 2.
- [Bou86b] J. Bourgain. “On high dimensional maximal functions associated to convex bodies”. *American Journal of Mathematics* 108.6 (1986), pp. 1467–1476.
- [Che21] Y. Chen. “An almost constant lower bound of the isoperimetric coefficient in the KLS conjecture”. *Geometric and Functional Analysis* 31 (2021), pp. 34–61.
- [CE22] Y. Chen and R. Eldan. “Localization schemes: A framework for proving mixing bounds for Markov chains”. In: *2022 IEEE 63rd Annual Symposium on Foundations of Computer Science (FOCS)*. IEEE, 2022, pp. 110–122.
- [CFM24] T. A. Courtade, M. Fathi, and D. Mikulincer. “Stochastic proof of the sharp symmetrized Talagrand inequality”. *Comptes Rendus. Mathématique* 362.G12 (2024), pp. 1779–1784.
- [Dem+25] E. Demyanenko, D. Straziota, C. Baldassi, and C. Lucibello. “Sampling through Algorithmic Diffusion in non-convex Perceptron problems”. *arXiv preprint arXiv:2502.16292* (2025).
- [DH12] F. Den Hollander. “Probability theory: The coupling method”. *Lecture notes available online* (2012).
- [Dur18] R. Durrett. *Stochastic calculus: a practical introduction*. CRC press, 2018.

- [EAMS22] A. El Alaoui, A. Montanari, and M. Sellke. “Sampling from the Sherrington-Kirkpatrick Gibbs measure via algorithmic stochastic localization”. In: *2022 IEEE 63rd Annual Symposium on Foundations of Computer Science (FOCS)*. IEEE. 2022, pp. 323–334.
- [Eld13] R. Eldan. “Thin shell implies spectral gap up to polylog via a stochastic localization scheme”. *Geometric and Functional Analysis* 23.2 (2013), pp. 532–569.
- [Eld16] R. Eldan. “Skorokhod embeddings via stochastic flows on the space of Gaussian measures”. In: *Annales de l’Institut Henri Poincaré-Probabilités et Statistiques*. Vol. 52. 3. 2016, pp. 1259–1280.
- [Eld20] R. Eldan. “Taming correlations through entropy-efficient measure decompositions with applications to mean-field approximation”. *Probability Theory and Related Fields* 176.3 (2020), pp. 737–755.
- [Eld22] R. Eldan. “Analysis of high-dimensional distributions using pathwise methods”. In: *Proc. Int. Cong. Math.* Vol. 6. 2022, pp. 4246–4270.
- [EKZ22] R. Eldan, F. Koehler, and O. Zeitouni. “A spectral condition for spectral gap: fast mixing in high-temperature Ising models”. *Probability theory and related fields* 182.3 (2022), pp. 1035–1051.
- [EL14] R. Eldan and J. Lehec. “Bounding the norm of a log-concave vector via thin-shell estimates”. In: *Geometric Aspects of Functional Analysis: Israel Seminar (GAFA) 2011-2013*. Springer. 2014, pp. 107–122.
- [EMZ20] R. Eldan, D. Mikulincer, and A. Zhai. “The CLT in high dimensions”. *The Annals of Probability* 48.5 (2020), pp. 2494–2524.
- [FÜ04] D. Feyel and A. S. Üstünel. “Monge-Kantorovitch measure transportation and Monge-Ampere equation on Wiener space”. *Probability theory and related fields* 128 (2004), pp. 347–385.
- [Föl88] H. Föllmer. “Random fields and diffusion processes”. *Lect. Notes Math* 1362 (1988), pp. 101–204.
- [GPC18] A. Genevay, G. Peyre, and M. Cuturi. “Learning Generative Models with Sinkhorn Divergences”. In: *Proceedings of the Twenty-First International Conference on Artificial Intelligence and Statistics*. Ed. by A. Storkey and F. Perez-Cruz. Vol. 84. Proceedings of Machine Learning Research. PMLR, 2018, pp. 1608–1617.
- [GS84] C. R. Givens and R. M. Shortt. “A class of Wasserstein metrics for probability distributions.” *Michigan Mathematical Journal* 31.2 (1984), pp. 231–240.
- [Gla04] P. Glasserman. *Monte Carlo Methods in Financial Engineering*. 2004.
- [Goo+14] I. J. Goodfellow, J. Pouget-Abadie, M. Mirza, B. Xu, D. Warde-Farley, S. Ozair, A. Courville, and Y. Bengio. “Generative Adversarial Nets”. In: *Advances in Neural Information Processing Systems*. Ed. by Z. Ghahramani, M. Welling, C. Cortes, N. Lawrence, and K. Weinberger. Vol. 27. Curran Associates, Inc., 2014.
- [Gre+24] L. Grenioux, M. Noble, M. Gabrié, and A. O. Durmus. “Stochastic Localization via Iterative Posterior Sampling”. In: *International Conference on Machine Learning*. PMLR. 2024, pp. 16337–16376.
- [Gua24] Q. Guan. “A note on Bourgain’s slicing problem”. *arXiv preprint arXiv:2412.09075* (2024).
- [HD05] A. Hyvärinen and P. Dayan. “Estimation of non-normalized statistical models by score matching.” *Journal of Machine Learning Research* 6.4 (2005).
- [JLV22] A. Jambulapati, Y. T. Lee, and S. S. Vempala. “A slightly improved bound for the KLS constant”. *arXiv preprint arXiv:2208.11644* (2022).
- [KLS95] R. Kannan, L. Lovász, and M. Simonovits. “Isoperimetric problems for convex bodies and a localization lemma”. *Discrete & Computational Geometry* 13 (1995), pp. 541–559.

- [KL22] B. Klartag and J. Lehec. “Bourgain’s slicing problem and KLS isoperimetry up to polylog”. *Geometric and functional analysis* 32.5 (2022), pp. 1134–1159.
- [KL24] B. Klartag and J. Lehec. “Affirmative Resolution of Bourgain’s Slicing Problem using Guan’s Bound”. *arXiv preprint arXiv:2412.15044* (2024).
- [KP23] B. Klartag and E. Putterman. “Spectral monotonicity under Gaussian convolution”. In: *Annales de la Faculté des sciences de Toulouse: Mathématiques*. Vol. 32. 5. 2023, pp. 939–967.
- [LV17] Y. T. Lee and S. S. Vempala. “Eldan’s stochastic localization and the KLS hyperplane conjecture: an improved lower bound for expansion”. In: *2017 IEEE 58th Annual Symposium on Foundations of Computer Science (FOCS)*. IEEE. 2017, pp. 998–1007.
- [Leh13] J. Lehec. “Representation formula for the entropy and functional inequalities”. In: *Annales de l’IHP Probabilités et statistiques*. Vol. 49. 3. 2013, pp. 885–899.
- [LS77] R. S. Lipster and A. N. Shiiriev. *Statistics of random processes I: general theory*. Springer-Verlag, 1977.
- [LS93] L. Lovász and M. Simonovits. “Random walks in a convex body and an improved volume algorithm”. *Random structures & algorithms* 4.4 (1993), pp. 359–412.
- [MS24] D. Mikulincer and Y. Shenfeld. “The Brownian transport map”. *Probability Theory and Related Fields* 190.1 (2024), pp. 379–444.
- [Mon23] A. Montanari. “Sampling, diffusions, and stochastic localization”. *arXiv preprint arXiv:2305.10690* (2023).
- [MW23] A. Montanari and Y. Wu. “Posterior sampling from the spiked models via diffusion processes”. *arXiv preprint arXiv:2304.11449* (2023).
- [Nad+19] K. Nadjahi, A. Durmus, U. Simsekli, and R. Badeau. “Asymptotic guarantees for learning generative models with the sliced-Wasserstein distance”. *Advances in Neural Information Processing Systems* 32 (2019).
- [Øks03] B. Øksendal. *Stochastic differential equations*. Springer, 2003.
- [Rob92] H. E. Robbins. “An empirical Bayes approach to statistics”. In: *Breakthroughs in Statistics: Foundations and basic theory*. Springer, 1992, pp. 388–394.
- [Sal+18] T. Salimans, H. Zhang, A. Radford, and D. Metaxas. “Improving GANs Using Optimal Transport”. In: *International Conference on Learning Representations*. 2018.
- [Son+20] Y. Song, J. Sohl-Dickstein, D. P. Kingma, A. Kumar, S. Ermon, and B. Poole. “Score-based generative modeling through stochastic differential equations”. *arXiv preprint arXiv:2011.13456* (2020).
- [TZ24] W. Tang and H. Zhao. “Score-based Diffusion Models via Stochastic Differential Equations—a Technical Tutorial”. *arXiv preprint arXiv:2402.07487* (2024).
- [TZ+07] P. K. Trivedi, D. M. Zimmer, et al. “Copula modeling: an introduction for practitioners”. *Foundations and Trends® in Econometrics* 1.1 (2007), pp. 1–111.
- [Vir+20] P. Virtanen et al. “SciPy 1.0: fundamental algorithms for scientific computing in Python”. *Nature methods* 17.3 (2020), pp. 261–272.
- [WW16] B. Wang and R. Wang. “Joint mixability”. *Mathematics of Operations Research* 41.3 (2016), pp. 808–826.